

https://dspace.org/

A polarographic and potentiometric study of metal-ligand equilibria: Instrumentation and investigations of systems with non-reversible electrode reactions

Mkwizu, Tumaini Samuel Peter

2006-11-13T13:05:09Z
http://hdl.handle.net/10539/1647

Downloaded from a DSpace repository. https://dspace.org/

CHAPTER 4

DEVELOPMENT OF AUTOMATED INSTRUMENTATION

4.1 INTRODUCTION

This chapter provides detailed information on the development of a dedicated computer–controlled instrumental set–up, capable of automated titrations whereby potentiometric and/or sampled direct current polarographic measurements are made on a given sample solution. In particular, the instrumental set–up has been applied in collection of glass electrode potentiometric as well as sampled direct current polarographic data in experiments involving studies of protonation equilibria (GEP only) and metal–ligand equilibria (GEP and DCP) at fixed L_T : M_T ratio and variable pH.

Automation of a given process would typically involve identification of the necessary hardware and software to be developed for controlling the process, with partial or full elimination of human intervention. In general, the need for automating a given process or experimental method requires initial consideration of the following possibilities:

a) Is a commercial instrument available to perform the analysis?
b) Can any commercial instrument be modified to perform the analysis?
c) If neither (a) nor (b) applies, is the design and development of a new automated process economically and technically feasible?

An affirmative answer to (c) generates an applied research project to design, build and test an automatic system with required capabilities [1].

As highlighted in the introductory chapter, the first aim in this project involved development of a computer-controlled, instrumental set–up which can be applied for, (i) automated potentiometric measurements on a given solution sample; (ii) automated polarographic measurements in metal–ligand equilibria studies at fixed ligand to metal concentration ratios and variable pH. With regards to commercial

availability of an automated potentiometric titrator, there are many such titrators as highlighted in the introductory chapter. The main question is can such commercial instruments be easily modified to incorporate automated polarographic measurements as required for metal-ligand equilibria studies at fixed L_T : M_T ratios and varied pH? Unfortunately, the answer is no. Commercially-available automatic potentiometric titrators cannot be modified easily to incorporate polarographic measurements.

As far as the initial considerations outlined above are concerned, the development of an automated potentiometric titration system in this project was justifiable simply because of the need for automated polarographic measurements at fixed L_T : M_T ratios and variable pH, since such experiments are necessarily accompanied by pH measurements, which are potentiometric in nature (whereby a glass electrode is used as an indicator electrode).

So, how does one go about developing instrumentation with the capabilities required as output from this project? The proposed solution in this project was to apply the concept of *virtual instrumentation*.

4.1.1 General Concepts on Virtual Instrumentation

A virtual instrumentation system can be regarded as computer software that a user would employ to develop a computerized measurement system, for controlling (from a computer screen) an external measurement hardware device, and for displaying or storing the measured data collected by the external device [2]. Virtual instrumentation can simply be defined as combining hardware and software with industry–standard computer technologies to create user-defined instrumentation solutions. In virtual instruments, the same set of stand–alone hardware components can perform different tasks imposed on them by the software [3].

The recent developments in the field of instrumentation have changed the principles of instrument design and construction since the software becomes the

actual “instrument” (the so called “virtual instrument” or VI). So, instead of dedicated real instruments, a personal computer, equipped with a multifunction Data Acquisition (DAQ)[1] card (or appropriate interfacing devices) and appropriate software, is turned into a flexible instrument capable of controlling a variety of experiments with acquisition of required raw data [4–5]. The primary benefits of applying data acquisition technology to configure virtual instrumentation include costs, size, flexibility and ease of programming. It has been estimated that the cost to configure a virtual instrumentation system using a data acquisition board or cards can be as little as 25% of the cost of a conventional instrument [6].

The flexibility of using virtual instrumentation can be found in a graphical programming software package known as LabVIEW. LabVIEW is an acronym for Laboratory Virtual Instrument Engineering Workbench. LabVIEW is an object–oriented graphical programming software package developed by National Instruments [6]. LabVIEW is a general–purpose programming environment designed as a complete set of applications for instrument and process control, data acquisition and scientific computing, including simulation and data analysis. Each program (called Virtual Instrument or VI) is composed of two levels: (i) the front panel, which is the graphical user interface (GUI) containing controls for input operations and indicators for output operations, and (ii) the graphical block diagram in which the actual programming code is structured by interconnecting icons representing mathematical operators, values and logic actions [7].

With regards to technical feasibility in the development of the dedicated computer–controlled instrumentation envisaged in this project, LabVIEW was chosen as the platform for development of the necessary software. LabVIEW’s graphical programming environment makes it easy to use and realistic for someone without any programming experience to learn programming quickly

[1] Data Acquisition (DAQ) is the means by which physical signals, such as voltage, current, pressure, and temperature, are converted into digital formats and brought into a computer. DAQ devices are devices that connect to the computer allowing the user to retrieve digitized data values. These devices typically connect directly to the computer’s internal bus through a plug–in slot. The DAQ devices convert the incoming signal into a digital form that is sent to the computer. The DAQ device does not compute or calculate the final measurement. This task is left to the software that resides in the computer [2].

enough to develop virtual instruments for use in desired computer–controlled experiments.

4.2 DESCRIPTION OF THE HARDWARE

A block diagram of the instrumental set–up for automated potentiometric and polarographic measurements is illustrated in Figure 4.1. The instrumental set-up can be regarded as essentially being composed of seven main components:

(1) Data collection and processing interface.
(2) An electronic control box.
(3) Digital pH meter.
(4) Digital burette.
(5) Magnetic stirrer.
(6) Potentiostat and current–measuring system.
(7) Voltammetric stand.

In Figure 4.2, a circuit diagram depicting the interfacing and connectivity of the various hardware components comprising the potentiometric–polarographic instrumental set–up developed is shown. Detail descriptions of the circuitry and interfacing hardware are presented in the following subsections (4.2.1 – 4.2.7). Supplementary information for the description of the instrumental set–up has been documented in Appendix A.

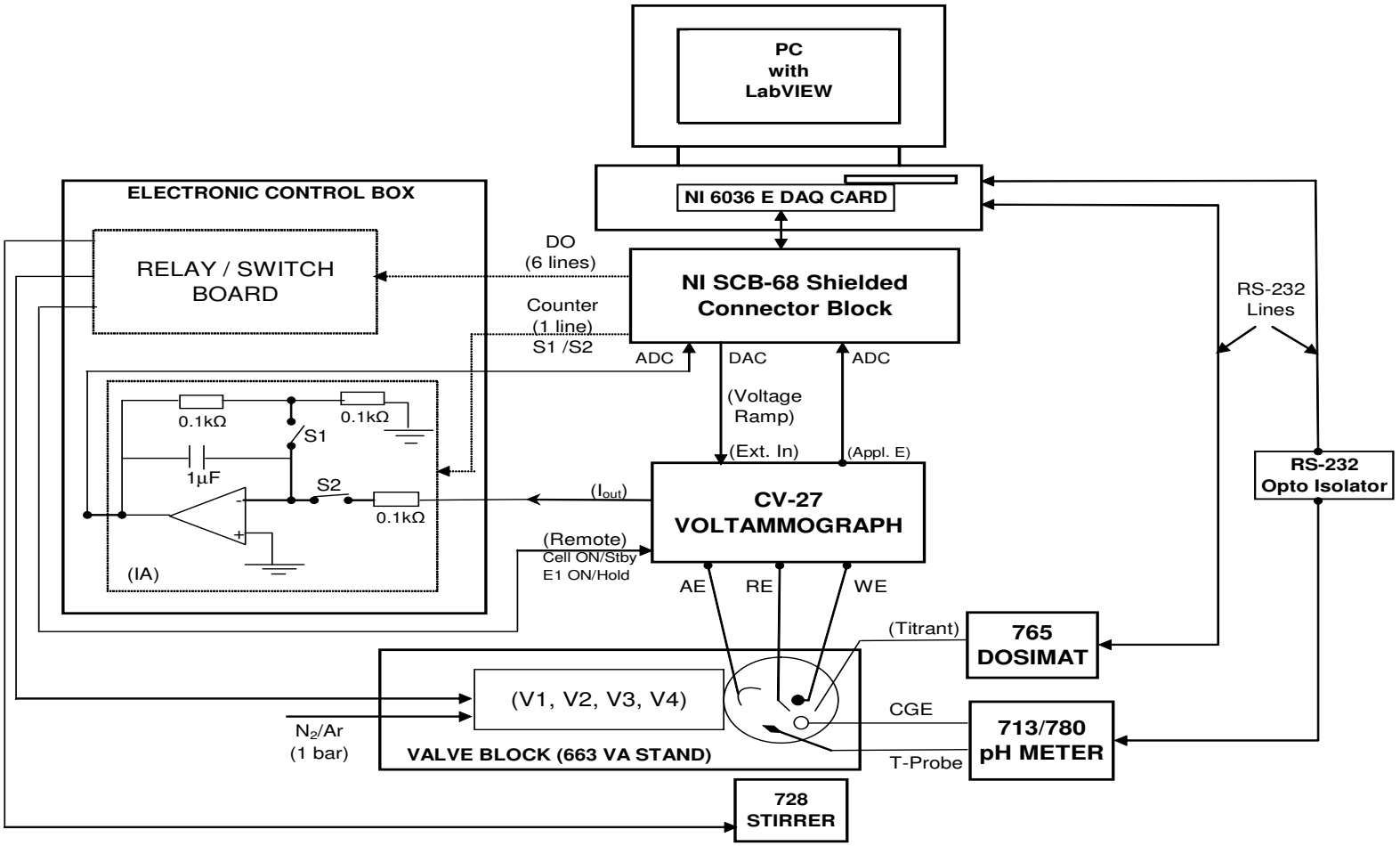


Figure 4.1: A block diagram showing interfacing and connectivity of the various hardware components of the instrumental set–up for potentiometric and polarographic measurements. CGE = Combination Glass Electrode; AE = Auxilliary Electrode; RE = Reference Electrode; WE = Working Electrode; T–Probe = Temperature Probe; ADC = Analog–to–Digital Converter; DAC = Digital–to–Analog Converter; DO = Digital Output; IA = Integration Amplifier; V1, V2, V3, V4 are solenoid valves on the valve block of the 663 VA stand (See Appendix A for more details and explanation of the symbols and abbreviations used).

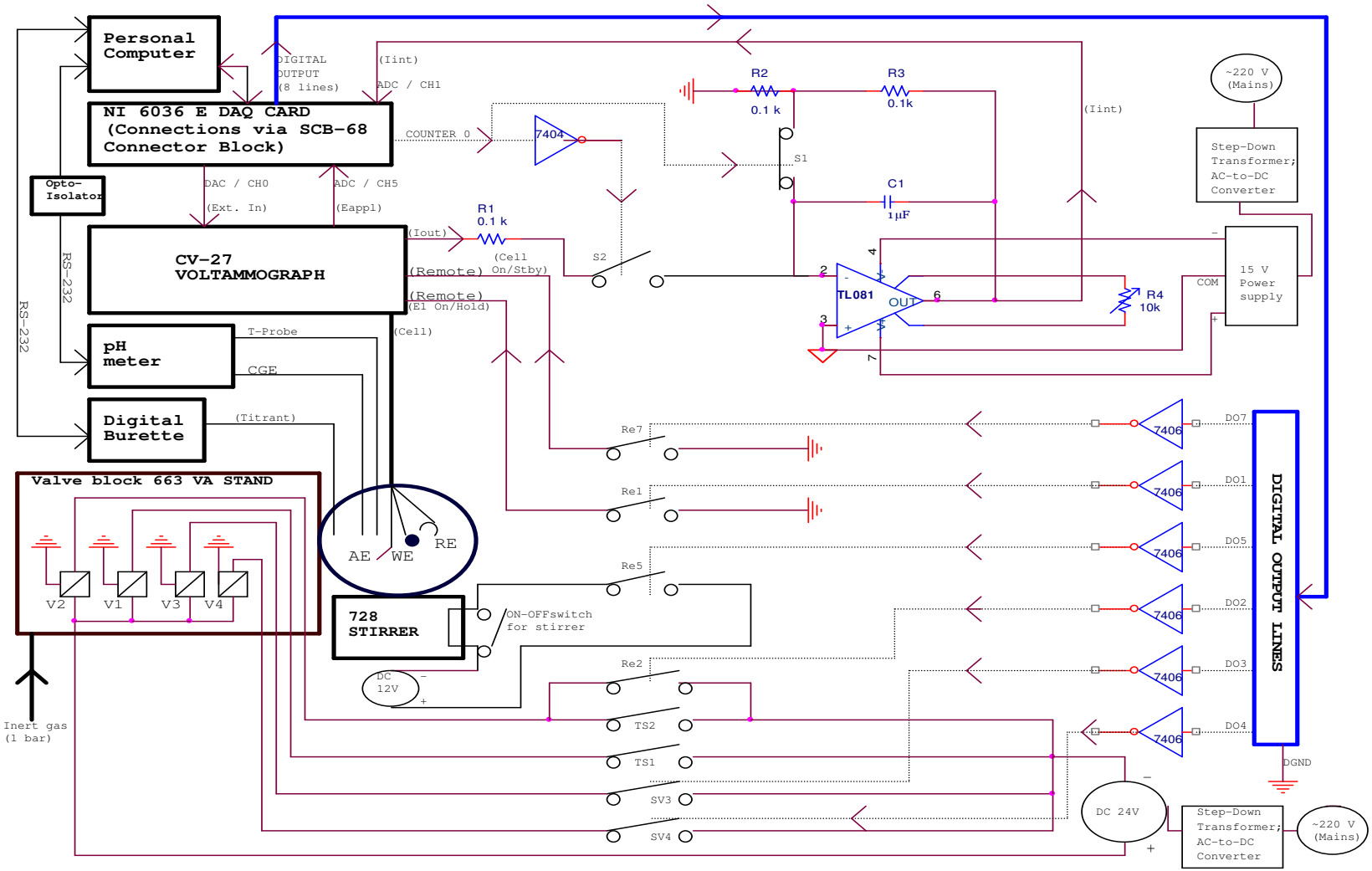


Figure 4.2: A simplified circuit diagram showing connectivity and interfacing of the electronic components used in the instrumentation for automated DC polarographic and potentiometric measurements (see text and Table A.1 (in Appendix A) for more details and explanation of the symbols and abbreviations used).

4.2.1 Data collection and processing interface

The data collection and processing interface of the instrumentation comprised of a personal computer (PC) equipped with serial communication ports (using RS–232 protocols) and a Data Acquisition Card (or DAQ card). Serial communication is a popular means of transmitting data between a computer and a peripheral device such as a programmable instrument or another computer. Serial communication uses a transmitter to send data, one bit at a time, over a single communication line to a receiver. Serial communication is popular because most computers have one or more serial ports, so no extra hardware is needed other than a cable to connect the instrument to the computer [2].

The PC used to control the instrumental set–up ran with Intel Pentium III or Intel Pentium IV as central processing units. The PC was equipped with LabVIEW full–development software package version 7.0 (National Instruments, Austin, Texas, USA). Windows 2000 or Windows XP (Microsoft, Seattle, Washington, USA) were used as the operating platforms of the personal computer. The DAQ card used was type NI 6036 E (National Instruments, Austin, Texas, USA) that was installed (as a plug–and–play hardware) in a special slot (a PCI slot) of the motherboard of the PC. The NI 6036 DAQ card is a multifunction device with the following operational characteristics:

- 16 single–ended or 8 differential Analog Input (AI) channels (software–selectable per channel) multiplexed to a 16–bit Analog–to–Digital Converter (ADC) with a ±10 V operating range;
- 2 Analog Output (AO) channels multiplexed to a 16–bit Digital–to–Analog Converter (DAC) with a ±10 V operating range;
- The ADC and DAC have a guaranteed maximum sampling rate of 200 kHz;
- 8 Digital Input/Output channels; and
- Two 24–bit counter channels for high precision and time–critical measurements with base clock frequency of 20 MHz.

A shielded connector block (SCB–68 from National Instruments, Austin, Texas, USA) has been used for easy connection of all analog and digital signals to and from the DAQ card.

It was found necessary to use an RS–232 optical isolation module to isolate the pH meter electronics from the rest of the instrumentation (see Figures 4.1 and 4.2). Optical isolation modules (commonly known as opto–isolators) provide communication links that have no electrical connections from one serial port to the other. This kind of isolation is important if a system uses electrical components that have different power sources or must operate at different ground potentials. In the instrumental set–up developed in this project, an RS–232 Opto Isolator model DLP 510 (Clearline, South Africa) was used.

4.2.2 Electronic Control Box

A metallic–shielded electronic control box was built in–house. The electronic control box contained the necessary additional electronics that were required to achieve computer–control of the commercial hardware components used in the instrumental set–up developed. It consisted of:

i. DC power supply units (5V, 15V and 24V) derived from the mains AC power supply (~220 V) and utilizing step–down transformers and AC–to–DC converters.
ii. Reed relays[2].
iii. Digitally–controlled ON–OFF switches.
iv. Manually–controlled ON–OFF switches.
v. An integration amplifier circuitry.

The specific details of the above–mentioned electrical hardware components have been described in subsequent subsections in conjunction with descriptions of the commercial hardware components that they have been interfaced to.

[2] Reed relays are electrically operated switches where a magnetic field created by current flowing through a coil results in a magnet being pushed to close the switch contacts [9]. All reed relays used in the instrumentation developed were standard type D31A31 (Celduc Relais, Sorbiers, France).

4.2.3 Digital pH meter

Either model 713 or 780 pH meters (Metrohm, Herisau, Switzerland) could be interchangeably used for potentiometric and temperature measurements. The pH meters could be set to do potential measurements in mV, direct pH measurements, and temperature measurements. The pH meters were of high quality with resolutions of ± 0.1 mV (± 0.001 pH units) for potentiometric measurements and ± 0.1 ° C for temperature measurements. The main feature of interest to their use in the development of the instrumental set–up was that they have an extensive remote control facility that allows full computer–control of the instruments via the RS–232 interface [8].

The pH meter was connected (using an RS–232 cable) to the controlling personal computer through one of the available serial ports (RS–232 COM port). The dedicated virtual instrument software modules (for sampling data from the pH meter) were instructed to gather data from the serial port. Since the pH meter was connected in this manner, there was no discrepancy in the data taken from the pH meter. The software received the same two or three decimal floating-point numbers seen on the pH meter's display.

4.2.4 Digital burette

The digital burette (used for automated titrant additions) was selected such that (i) it could be interfaced to a personal computer using RS–232 protocols without need for modification or any additional interfacing components, and (ii) it would be commercially–available at a reasonable cost.

A model 765 Dosimat (Metrohm) was found to be a suitable digital burette for the instrumental set–up. The 765 Dosimat could be computer–controlled using its RS–232 interface connector. When using the 765 Dosimat manually, one uses a small keyboard for operation. All the functions of the 765 Dosimat, such as, dosing mode, volume increment, dosing rate etc., could be implemented for remote control via a PC using appropriate RS–232 commands provided by the

manufacturer in the documentation for operating instructions [10]. In addition, the RS–232 communication to the 765 Dosimat is bidirectional, i.e., the digital burette can be instructed to perform appropriate operations remotely and the burette can send data to the controlling computer. Since, the 765 Dosimat was serially connected to the PC, the controlling software could gather data from it without any discrepancy.

Table 4.1 Some specifications for the burette cylinders (exchange units) used with a 765 Dosimat (digital burette)

Exchange unit	Resolution		Smallest volume increment
	Volume / mL	Rate mL/min	
1 mL	0.001	0.001	0.1 μL
5 mL	0.001	0.005	0.5 μL
10 mL	0.001	0.010	1 μL
20 mL	0.002	0.020	2 μL

Another advantage of using the 765 Dosimat was that it could be used, in a very flexible manner, with different burette cylinders (known as Exchange Units) of varying maximum capacity (1 mL, 5 mL, 10 mL, 20 mL, or 50 mL). Depending on the accuracy of volume additions desired, the user would select the appropriate exchange unit for his/her application. Table 4.1 shows some specifications of the various exchange units available for use with the 765 Dosimat.

4.2.5 Magnetic stirrer

The magnetic stirrer used for mixing sample solutions was a model 728 Magnetic Stirrer (Metrohm, Herisau, Switzerland). The stirring rate was controlled manually using a knob on the front panel of the stirrer. The scale of the stirring rate was from 1 to 10. Position 1 corresponded to the minimum stirring rate (200 revolutions/minute), and position 10 corresponded to the maximum stirring rate (1900 revolutions/minute). The 728 Magnetic Stirrer required an operational voltage of a DC voltage of +5 to +12 V. A standard power adapter (Metrohm,

Output: +12 V DC, Input: 200 – 240 V AC) was used to power the stirrer. For computer–control, the ON–OFF status of the magnetic stirrer was achieved via a digitally–controlled reed relay Re5 resident in the electronic control box. The ON–OFF state of Re5 was operated using a computer–generated digital TTL[3] signal from Digital Output line 5 of the DAQ card. The reed relay Re5 was connected *in series* with the manually–operated ON–OFF switch on the front panel of the stirrer (which was always kept "ON" during operation of the instrumentation). This arrangement ensured that during execution of a potentiometric–polarographic experiment, the ON–OFF state of the stirrer was computer–controlled via the reed relay Re5 only (see Figure 4.2).

The stirrer could be operated via the 713 pH meter or the 765 Dosimat, but the computer–control of the stirrer via digital TTL signals from the DAQ card, was more desirable in this case as it allowed for flexibility in using the same set of hardware components for polarographic as well as potentiometric measurements. In potentiometry, the sample solution must be stirred all the time during measurements. In polarography, the sample solution is stirred to achieve homogeneous equilibration, followed by polarographic measurements of a static solution to ensure diffusion–controlled processes at the electrode surface.

4.2.6 Potentiostat and current–measuring system

A CV–27 Voltammograph (Bioanalytical Systems, Indiana, USA) was used as a potentiostat. The CV–27 voltammograph (abbreviated as CV–27) is a flexible device capable of controlled potential experiments, potential measurements at zero current, and charge measurement experiments. Electronic functions integrated into the CV–27 include (i) a potentiostat (± 5.00 V applied potential, ±10 V compliance, 120 mA maximum current); (ii) a linear ramp and pulse waveform generator; (iii) an ability to bring an external waveform directly into the potentiostat (via a built–in summing point); and (iv) a current–to–voltage converter with gain (0.002 mA/V to 10 mA/V). Every controlled parameter and

[3] TTL signals are square–pulse signals that have two states, i.e., 0 V (low) or 5 V (high) [2].

output variable, may be read, in the proper units of measure, on the $3^{1/2}$ digit front panel display. Furthermore, all the control functions can be actuated by a separate, remote timer using TTL signals [11].

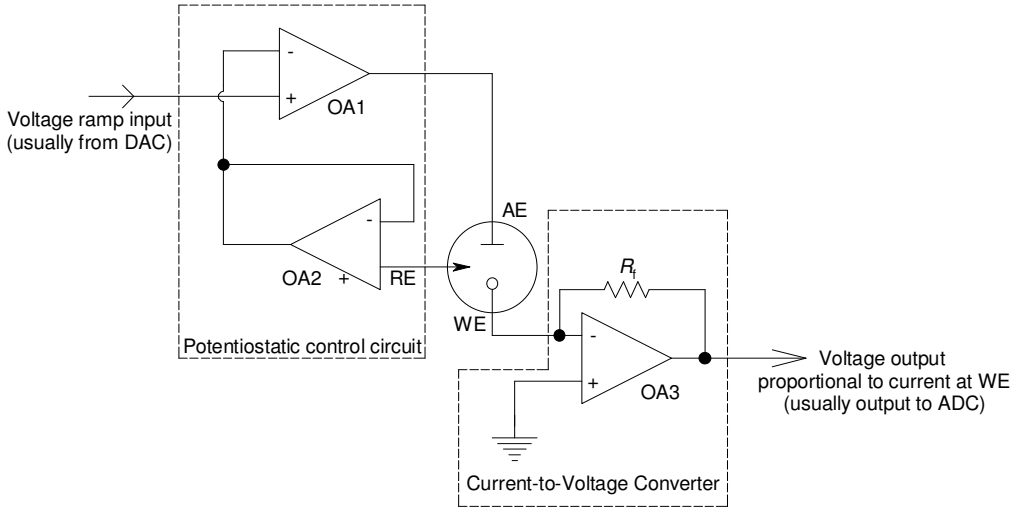


Figure 4.3: A basic potentiostatic three–electrode system with measurement of cell current via a current–to–voltage converter. OA = Operational amplifier.

A basic potentiostat circuit is shown in Figure 4.3. The potentiostat is usually made from three operational amplifiers. The top amplifier (OA1) usually receives the output from the digital–to–analog converter (DAC) as a voltage ramp and applies it to the auxiliary electrode in the electrochemical cell. The reference electrode probes the voltage applied between the AE and the working electrode, picking off a fraction of it close to the WE. This voltage is applied to the second operational amplifier (OA2). The OA2 plus the resistance between the AE and the RE form the feedback loop for the OA1. This sets the voltage applied to the working electrode to be essentially the same as the output of the DAC, no matter what the solution or reference electrode resistances are.

Current flowing through the electrochemical cell (between the WE and the AE) is converted into a voltage suitable for recording using the circuitry known as current–to–voltage converter (or current follower). The output voltage from the operational amplifier (OA3) used in the current follower circuitry is proportional to the input current by a scale factor determined by the resistor R_f (usually this

resistor is a variable resistor with an adjustable value that is varied to achieve desired sensitivity (or gain) [12].

In the instrumental system developed in this project, the voltage waveform for Sampled DC polarography was digitally generated by using a dedicated subprogram forming part of the software module for polarographic measurements (details have been presented in section 4.3.2). Each potential of the digital waveform was converted to an analog potential via one of the DAC channels (Analog Output channel 0) of the DAQ card (abbreviated as DAC / CH0 or DAC0OUT). The potential was then applied to the working electrode through the summing point of the CV–27 voltammograph (the input jack *Ext. In*, on the back panel of the CV–27, is used as input for an external waveform to the summing point of the CV–27 potentiostatic circuitry). The CV–27 measured the actual applied potential (E_{appl}) at the electrochemical cell. The corresponding current response (converted to a proportional voltage by the current–to–voltage converter of the CV–27) and the resulting analog signal was further amplified (to increase sensitivity) using a custom–built Integration Amplifier (IA) circuitry residing in the electronic control box. The integration amplifier circuitry is illustrated in Figure 4.4 (This circuitry is a section of the overall circuitry shown in Figures 4.1 and 4.2).

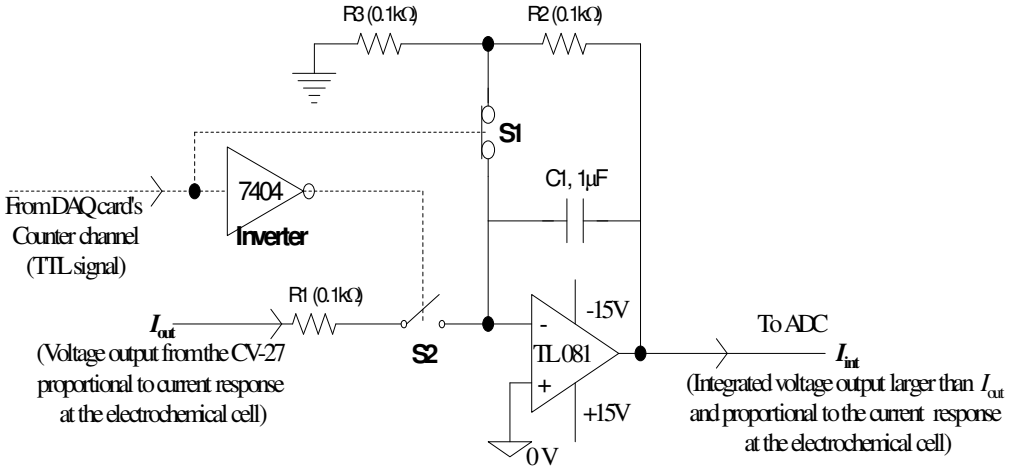


Figure 4.4: The integration amplifier circuitry used for amplification of the current response signals measured by the CV–27 voltammograph.

The integration amplifier circuitry was built by using a TL081 operational amplifier chip (National Semiconductor Corporation, California, USA) that was powered by 15 V using a custom–built power supply unit placed in the electronic control box. The 0 V (or COM) of the 15V power supply unit was used as a floating–ground for (+) input of TL081 operational amplifier. The operational amplifier, combined with a 1μF capacitor (C1) and 0.1 kΩ resistors R1, R2, and R3, as shown in the circuit diagram in Figure 4.4, can be regarded as being used to electronically calculate the integral of the input signal from the CV–27 (I_{out}). The output signal from the integration amplifier circuitry (I_{int}) is larger than the input signal and proportional to the input signal (the magnitude being determined by the time of integration). The overall control of the integration process was achieved by digitally controlling two ON–OFF electronic switches S1 and S2 (in a model SW-201 chip, Precision Monolithics, Massachusetts, USA) simultaneously. The S1 and S2 were controlled to work in an opposite fashion, i.e., if S1 was "ON", then S2 was set to "OFF" and vice versa. S2 was used to start the integration (when set to "ON"). S1 was used to reset the integration amplifier by discharging the capacitor C1 (a pathway to ground was provided when S1 was set to "ON").
One counter[4] channel (Counter 0 of the DAQ card) was used for simultaneous digital control of the switches S1 and S2. The ON–OFF state of these switches require TTL logic whereby a TTL low (0V) set the switches to "ON" and a TTL high (5V) set the switches to their "OFF" state. To achieve the ON–OFF operation of S1 and S2, an inverter[5] (type 7404 Hex inverter, Phillips Semiconductor Ltd, Frankfurt, Germany) was used to change the state of the TTL signal (sent via Counter 0) before it was passed to S2.

The TTL pulses from Counter 0 were also used to trigger the acquisition of the current response signals (output of the integration amplifier I_{int}) and applied potentials, E_{appl} (measured by the CV–27). The data acquisition of the E_{appl} values was undertaken using one of the ADC channels (Analog Input channel 5) of the

[4] Counters add counting or high–precision timing to a DAQ system. They respond to and output TTL signals that are 0 V (low) or 5 V (high) in value [2].
[5] An inverter is a device that changes the logic state of an input TTL signal. If the input signal is low (0V) the output signal is high (5V) and vice versa [2].

DAQ card (abbreviated as ADC / CH5 or ACH5). The I_{int} signal was acquired via Analog Input Channel 1 (abbreviated as ADC / CH1 or ACH1) of the ADC of the DAQ card. The AI channels were configured in differential analog input mode [2]. Sampled DC polarographic measurements were achieved in a highly reproducible manner by the use of the counter channel of the DAQ card. The counter ensured highly reproducible and synchronized measurements of the current response and applied potentials at the dropping mercury electrode.

Two digital output (DO) lines (DO1 and DO7) from the DAQ card were used for computer–control of two control functions of the CV–27: (i) To connect the CV–27 electronics to the electrodes (Cell ON/STBY) and (ii) To activate the potentiostatic mode of the CV–27 (E1 ON/Hold). Cell ON position connects the electrodes to the CV–27 electronics, and Cell STBY disconnects the cell from the CV–27 electronics. E1 ON applies a potential to the cell and with E1 HOLD, the working electrode is kept at the applied potential that is fixed at the desired value. Essentially, the E1 ON/HOLD controls the potentiostatic mode of the CV–27. For activation of these control functions, two digitally–controlled reed relays, Re1 and Re7, were used (See Figure 4.2).

Digital control of the CV–27 control functions was achieved using a 15–pin connector, called *Remote*, at the back panel of the CV–27. For remote control of the Cell ON/STBY function, pin 3 was used. For remote control of the E1 ON/HOLD pin 5 was used. Pin 1 was connected to digital ground (DGND). Any contact closure of pin 3 and pin 5 to ground, activated the control functions. The input signal to the reed relays Re1 and Re7 was DGND. The output signals of the Re1 and Re7 were connected to pin 5 and pin 3 of the 15-pin connector (Remote), respectively. The TTL signals from the digital output lines (DO1 and DO7) were inverted using type 7406 Hex Inverter (Phillips Semiconductor, MA, USA). The "ON" state of the reed relays (Re1 and Re7) required a low (0 V) TTL signal. The "OFF' state was triggered by a high (5 V) TTL signal. With the use of the 7406 inverters, the reed relays were set to "ON" by setting the digital output lines to high (5 V). The low (0 V) state of the digital output lines resulted in the reed relays being set to "OFF" (see Figure 4.2).

4.2.7 Voltammetric stand

Sampled DC Polarographic measurements were performed using the top part (the valve block) of a voltammetric stand (model 663 VA stand from Metrohm) equipped with a multi–mode electrode (MME) (Metrohm, Model 6.1246.020) as a working electrode. The MME consist of a mercury (Hg) reservoir and a glass capillary. The Hg reservoir flows through the glass capillary forming a drop at its end. The mercury flow is controlled by a sealing needle, which can be raised or lowered pneumatically using an inert gas supply (Nitrogen was used in this project and the required operating pressure of 1 ± 0.2 bar was set). The different types of electrodes (Hanging mercury drop electrode (HMDE), Dropping mercury electrode (DME), and Static mercury drop electrode (SMDE)) on the MME are implemented by timed opening or closing of the mercury flow using the sealing needle [13].

The operating characteristics of the valve block of the 663 VA stand and the MME are illustrated in Figure 4.5. The 663 VA stand has four solenoid valves[6] (V1, V2, V3, and V4) used for pneumatic control of the flow the inert gas (used for dearation of the sample solution and operation of the MME). Valve V1 allows flow of the inert gas to the entire valve block of the 663 VA stand. When valve V1 is activated, the mercury reservoir of the MME becomes pressurized. In standby mode there is the same pressure above and below the diaphragm of the sealing needle such that the sealing needle is pressed onto the glass capillary's top opening thus preventing the outflow of mercury from the gas capillary. The pressure above and below the sealing needle's diaphragm is provided via the inert gas feed lines 2 and 3 (see Figure 4.5). The sealing needle is a good electrical conductor and maintains electrical contact between the mercury drop and electrical connection to the potentiostat. The gas pressure above the sealing

[6] Solenoid valves are electro–mechanical devices that use a solenoid to control valve activation. A solenoid consists of a wire coil and a movable plunger that seat against the coil. When voltage is applied to the coil an actuating magnetic field is created that result in movement of the plunger which in turn activates the valve. When electrically energized or de–energized, solenoid valves either shut off or allow fluid flow [9].

needle's diaphragm is made to fall by switching over valve V3, whereupon the sealing needle lifts upwards and the mercury can flow out of the capillary.

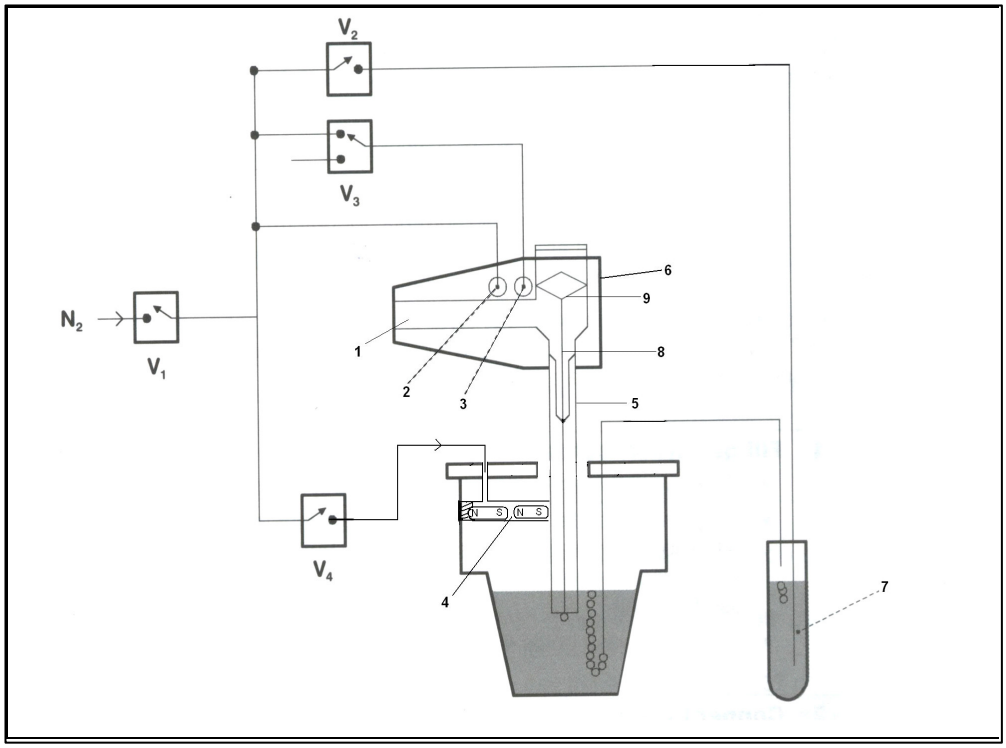


Figure 4.5: A schematic diagram showing the inert gas connections and operating principle of the valve block and multi–mode electrode of the 663 VA stand.
1 = Mercury reservoir; 2 = connection for inert gas supply of the MME for raising and lowering the sealing needle; 3 = connection for inert gas supply of the MME for pressurizing the mercury; 4 = Rapping magnet used as drop knocker; 5 = Glass capillary; 6 = Multi–mode electrode (MME); 7 = Gas wash bottle for inert gas supply; 8 = Sealing needle. V1, V2, V3, and V4 are the solenoid valves on the valve block of the 663 VA stand; 9 = Sealing needle's diaphragm.

Valve V2 is used to control passage of the inert gas to deaerate the sample solution. The tapping mechanism (operation of the drop knocker to allow formation of new mercury drops) of the VA stand is triggered by brief opening and closing of valve V4. When valve V4 is switched on, gas passes into the chamber with a rapping magnet that is accelerated towards the capillary. This impact is sufficient to separate the mercury droplet from the capillary tip [13].

In the computer–controlled instrumental set–up developed in this project, valves V1, V2, V3, V4 were activated by a 24 V DC voltage from a custom–built 24 V DC power supply unit (DC 24V) residing in the electronic control box. The passage of the 24 V DC voltage to the valves was controlled by switching ON–OFF dedicated switches and reed relays placed in the electronic control box.

Valve V1 was operated manually using a toggle switch (TS1) placed on the front panel of the electronic control box. Valve V1 (being the main valve for operation of the entire valve block of the 663 VA stand) was kept "ON" all the time, throughout an experiment.

Valve V2 was operated either manually using a toggle switch (TS2) on the front panel of the of the electronic control box or digitally via digital output line 2 (DO2) of the NI 6036 DAQ card which was used to switch ON–OFF a reed relay Re2. Switch TS2 and the relay Re2 were connected in parallel (see Figure 4.2). The dual operation of valve V2 provided some flexibility in dearation of solutions; manual operations that did not require invoking dedicated software. Computer–controlled operations, e.g. in automated polarographic measurements, the digitally–controlled relay Re2 was used for activating or deactivating valve V2. The parallel connection of the relay Re2 and the switch TS2 required the switch TS2 to be set "OFF" for all computer–controlled operations.

Valves V3 and V4 were digitally controlled via digital output line 3 (DO3) and digital output line 4 (DO4) of the NI 6036E DAQ card, respectively. Due to their time–critical nature (to achieve reproducibility in Sampled DC polarographic measurements), valves V3 and V4 were digitally–controlled via two solid–state, optically isolated switches named SV3 and SV4, respectively (type PCI–1109, Intelligent Instrumentation, Arizona, USA).

The TTL signals from all the digital lines used to operate the valves on the valve block of the 663 VA stand were inverted using 7406 Hex inverters (Phillips Semiconductor, MA, USA). The use of inverters allowed consistency in activating the TTL signals from the digital output lines to high (5 V) or low (0V) to

correspond with the ON or OFF status of the switches and relays used for operation of the valves.

A photograph of the instrumental set–up was presented in Figure 2.3 in Chapter 2 in conjunction with a discussion of the experimental procedures adopted in this project utilizing the instrumental set–up developed.

4.3 DESCRIPTION OF THE SOFTWARE

Various software modules (referred to as Virtual Instruments or VIs) for automated potentiometric experiments, polarographic experiments, or polarographic and potentiometric combined measurements, were developed. LabVIEW version 7.0 full–development programming package (National Instruments, Texas, USA) was used to develop the virtual instruments.

4.3.1 Potentiometry

Two main VIs were written for controlling experiments whereby only potentiometric measurements were made. The first VI was *Configure pH meter & Dosimat* and the second was *Autotitrator* (this was the main VI for automated potentiometric titrations with constant volume additions).

The VI *Configure pH meter & Dosimat* was used to configure the pH meter and the digital burette prior to execution of an automated titration. The VI was used to set the measuring mode (Temperature, pH or mV) and set the required precision of measured values (acquired by the pH meter) either to two or three decimal points. Furthermore, the VI was used to configure the 765 Dosimat for remote control operation using the computer. The remote control mode of the 765 Dosimat overrides manual operation of the digital burette. The required dosing mode for constant volume additions of the titrant, namely, Cumulative (DIS C), was selected. Moreover, the desired volume increment for each addition, with its corresponding dosing rate, was set using the *Configure pH meter & Dosimat*.

A flowchart showing the programmatic execution of the VI *Configure pH meter & Dosimat* is presented in Figure 4.6. Detailed descriptions of the software parameters have been documented separately in Table A.2 in Appendix A.

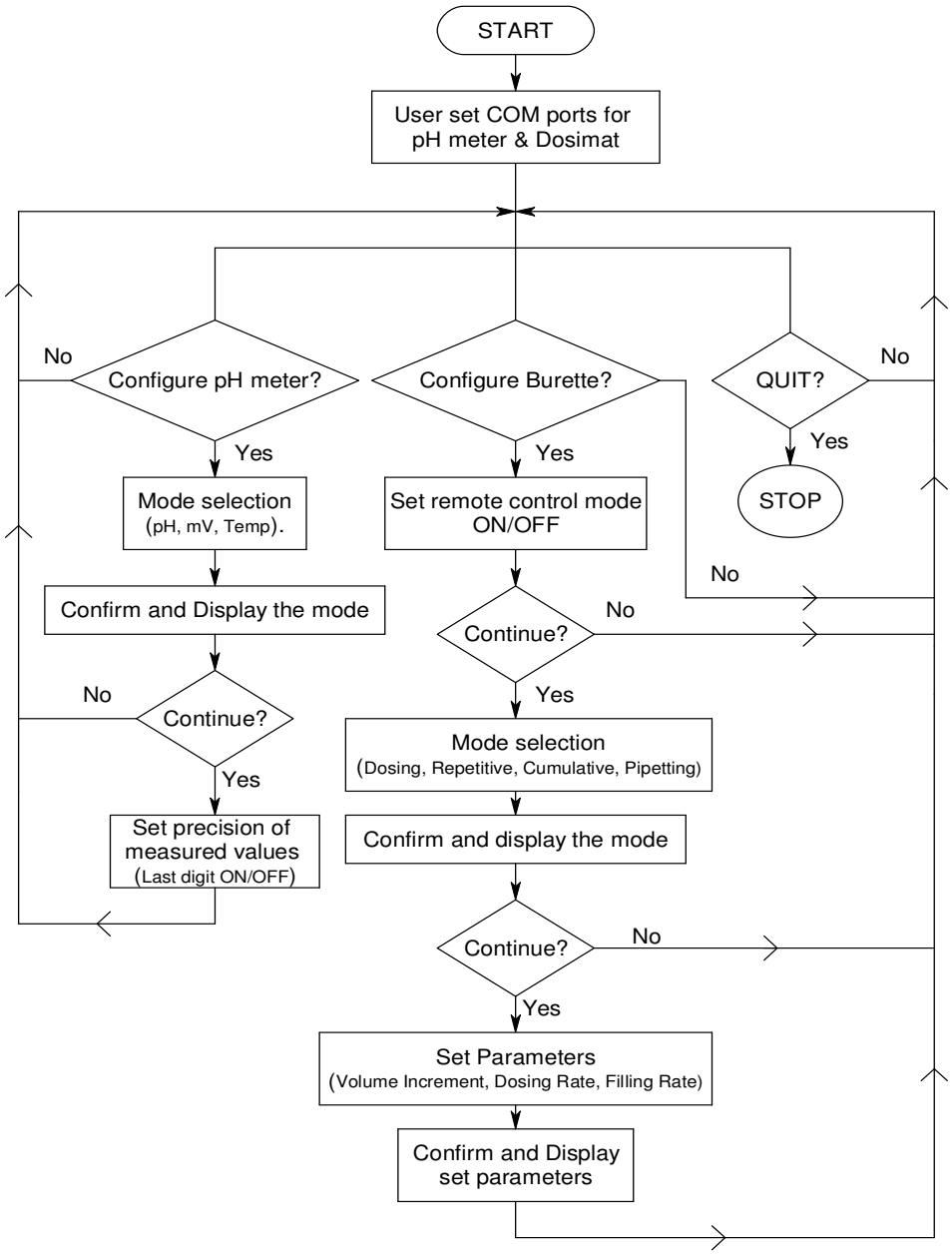


Figure 4.6: A flow chart of the *Configure Dosimat & pH meter VI* (the virtual instrument used to configure the pH meter and the digital burette (765 Dosimat) used in automated potentiometric–polarographic experiments).

The Autotitrator VI

The front panel (or the user–interface) of the virtual instrument *Autotitrator* is shown in Figure 4.7. Detailed descriptions of the software parameters have been documented separately in Table A.3 in Appendix A. Figure 4.8 represents a simplified flowchart which shows the way in which the *Autotitrator VI* executes programmatically.

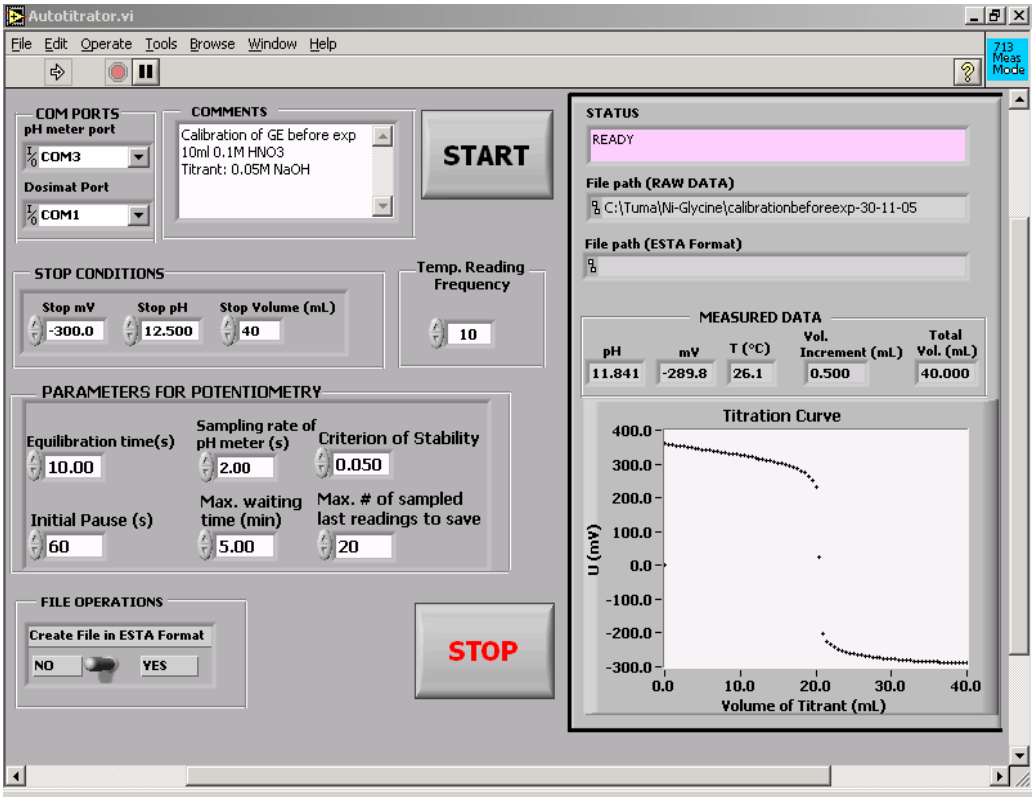


Figure 4.7: The front panel of the *Autotitrator VI*, the software module developed for automated potentiometric titrations with constant volume additions.

When performing an automated potentiometric titration using the *Autotitrator VI*, in the set of parameters called *STOP CONDITIONS*, the user enters three parameters, namely, S*top mV*, *Stop pH*, and *Stop Volume*. These parameters are used to automatically stop the *Autotitrator VI* from acquiring further data once any of the three conditions is met first. All stop conditions' parameters are programmatically checked at the end of each titration stage, i.e., before a new titrant increment is delivered to change solution composition.

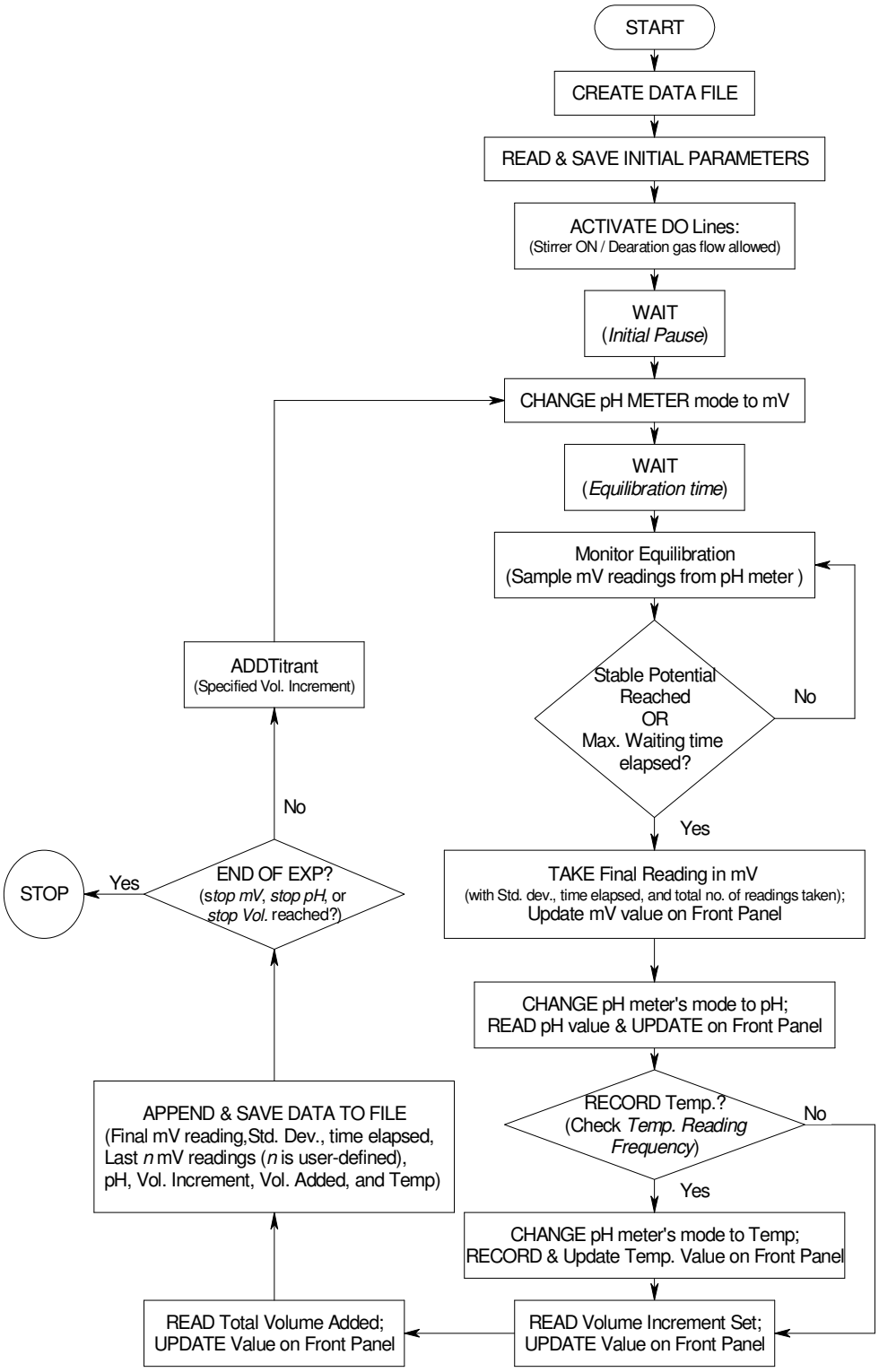


Figure 4.8: Flow chart of the *Autotitrator VI*, the virtual instrument for automated potentiometric titrations with constant volume additions. Temp. = Temperature; Std. dev. = Standard Deviation, Vol. = Volume; EXP = Experiment.

The *Autotitrator VI* was developed such that the user has freedom to guide how the automated titration should proceed as far as acquisition of stable potential readings is concerned. In the set of parameters called *PARAMETERS FOR POTENTIOMETRY*, the user defines how equilibrium potentials are to be gathered by the VI. The parameter *Initial Pause* is a time delay allowed to elapse at the beginning of a titration for the starting titrand solution to equilibrate after thorough mixing and purging. The parameter *Equilibration time* is a time delay that is allowed to elapse for equilibration to take place before the subroutine for checking this is loaded. For instance, for systems that the user knows equilibration is slow, there is freedom to allow for a long pause to elapse for equilibration to take place.

Determination of equilibrium potentials by the software

In any potentiometric titration, the electrode signal will not be stable immediately after a titrant increment has been delivered since it is influenced by the mixing speed and reaction rate in the solution and by the response of the electrode. In automated potentiometric titrations using the *Autotitrator VI*, equilibration is checked using a subroutine (or subVI) called *Sampling* 713/*780 pH* meter that is executed such that equilibrium potentials are evaluated in a statistical fashion by an iterative procedure. Each iteration is associated with acquisition of one potential reading from the pH meter. The user defines the S*ampling rate of the pH meter*, i.e., the time between successive potential readings sampled from the pH meter.

The algorithm for checking equilibration proceeds such that ten readings are successively sampled from the pH meter at the specified sampling rate. The ten potential readings are averaged arithmetically and the corresponding standard deviation calculated. This standard deviation, being a measure of spread of the potential readings as a function of time, is compared with the *Criterion of Stability*, which is a user–defined parameter. If the standard deviation of ten successive potential readings is less than the specified value of *Criterion of Stability*, then the subroutine for sampling the pH meter stops executing and the

final, “stable” reading is taken as the average of the last ten successive readings. The subroutine will repeat sampling new potential readings from the pH meter until the criterion of stability is achieved or the *Max. Waiting time*, that the user allowed, has elapsed. Figure 4.9 shows a flowchart of the subroutine *Sampling 713/780 pH meter*.

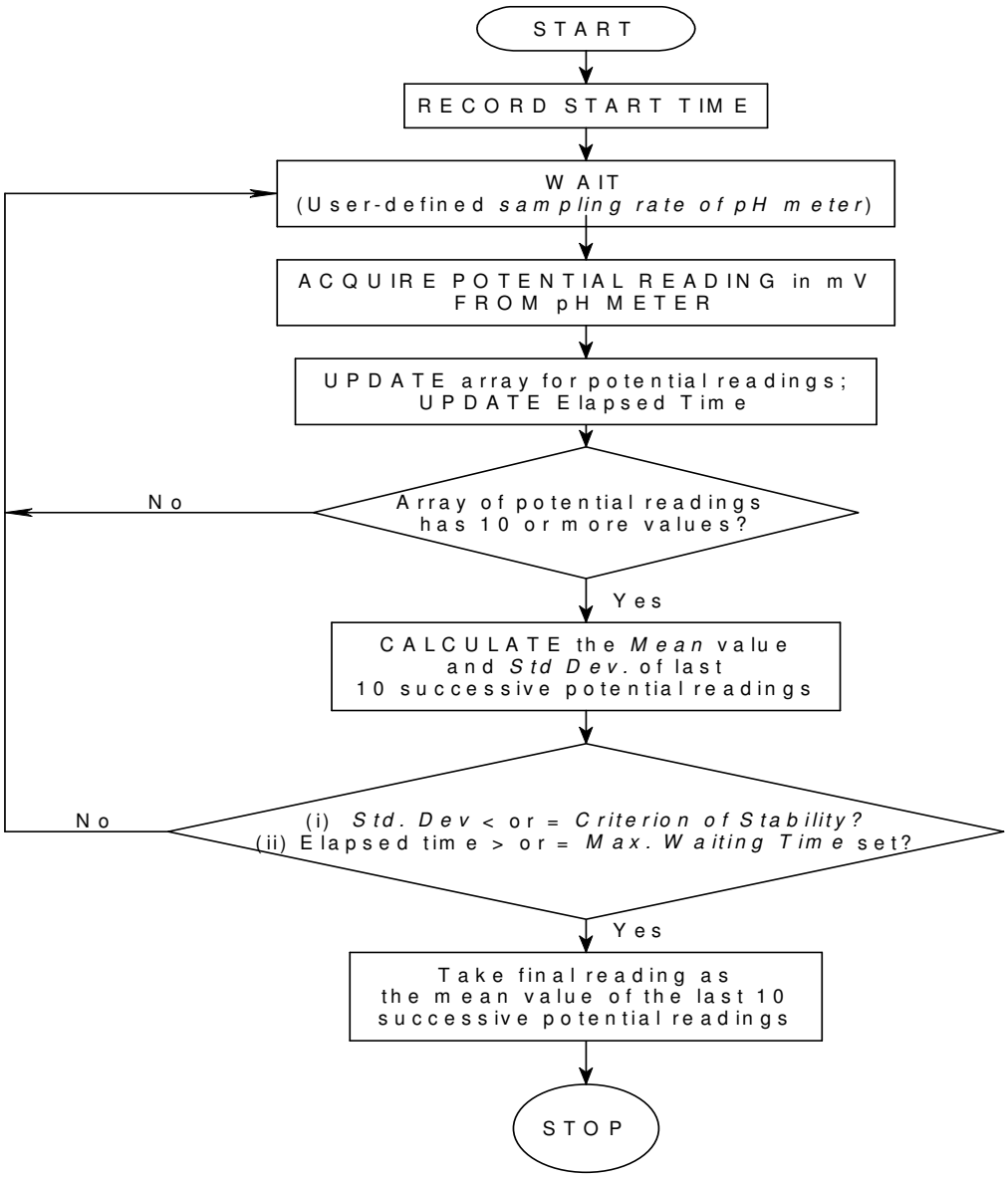


Figure 4.9: A flowchart of the subroutine (or SubVI) *Sampling 713/780 pH Meter* used to programmatically establish an equilibrium potential reading, at a particular titration stage, during an automated potentiometric titration.

Most automatic potentiometric titrators make use of a statistical average of sampled potential readings, at a specified sampling rate, in determination of the "equilibrated' potential reading at a certain titration stage [13–19].

Using the front panel input called *FILE OPERATIONS*; the operator opts for generation of a second raw data file that contains two columns: Volume of titrant (mL) and Potential (mV). The data in this second file are in a format required for data analysis using the ESTA suite of programs used for analysis of potentiometric data.

Progress of a given automated titration can be monitored by viewing several indicators that have been placed on the front panel of the *Autotitrator VI*. For instance, the *Titration Curve* gives the user some graphical information about changes in observed potentials as a titration progresses. The indicators are updated with every new potentiometric measurement made.

4.3.2 Sampled Direct Current Polarography

The virtual instrument for acquisition of one polarogram at a time is called *DC* (*One Polarogram*) *VI*. The virtual instrument controls the acquisition (and subsequent storage of data) of current developed from electrochemical processes at the DME and the corresponding actual applied potential. Furthermore, the VI generates appropriate waveform for voltage ramp to be applied to the cell via the CV–27 voltammograph.

The *DC* (*One Polarogram*) *VI* was principally developed as a prerequisite to the software modules for automated DCP measurements that are combined with potentiometric measurements on a sample solution whose composition is varied systematically by way of a titration (these software modules have been discussed later in section 4.3.3). Moreover, the *DC* (*One Polarogram) VI* could be used to acquire some preliminary DCP data on a given sample solution or polarograms of different sample solutions, whereby the user would manually change the composition of the sample solutions and acquire single DCP scans at his/her

discretion. For example, prior to performing an automated titration at a fixed L_T : M_T ratio in a study of a metal–ligand system by DCP, the user may have to record polarograms of the sample solution in the absence of the ligand using the *DC* (*One Polarogram*) *VI*.

The basic principles of sampled DC polarography were discussed in Chapter 1 (section 1.5.1). Basically, in carrying out DCP measurements under the control of the *DC* (*One Polarogram*) *VI*, the following functions are performed:

1) Sends the potential values and changes the set value of the potential of the DME linearly with time (strictly speaking the potentials are applied in a stepwise fashion).
2) Acquires and stores the response current (which is integrated) from the electrochemical cell.
3) Synchronizes the integration of the response current, measurement of resulting integrated response current and the applied potential (E_{appl}) with the mercury drop life.
4) Dislodges the mercury drop at fixed intervals.
5) Performs a real–time display of the DC wave adjusting automatically the current and E_{appl} axes.

The front panel of the *DC* (*ONE POLAROGRAM*) *VI* is shown in Figure 4.10. Detailed descriptions of the various parameters have been documented in Table A.4 (in Appendix A). The operator is able to select, via an input instruction, the drop time (*t-step*), the initial potential (*Initial E*), the final potential (*Final E*), the step potential (*E-step*), time of integration of the current response (*t-integration*), the time for dearation of the sample solution (*Purge time*), etc. After a scan is completed a dialogue box prompts the user whether to save the data acquired or not.

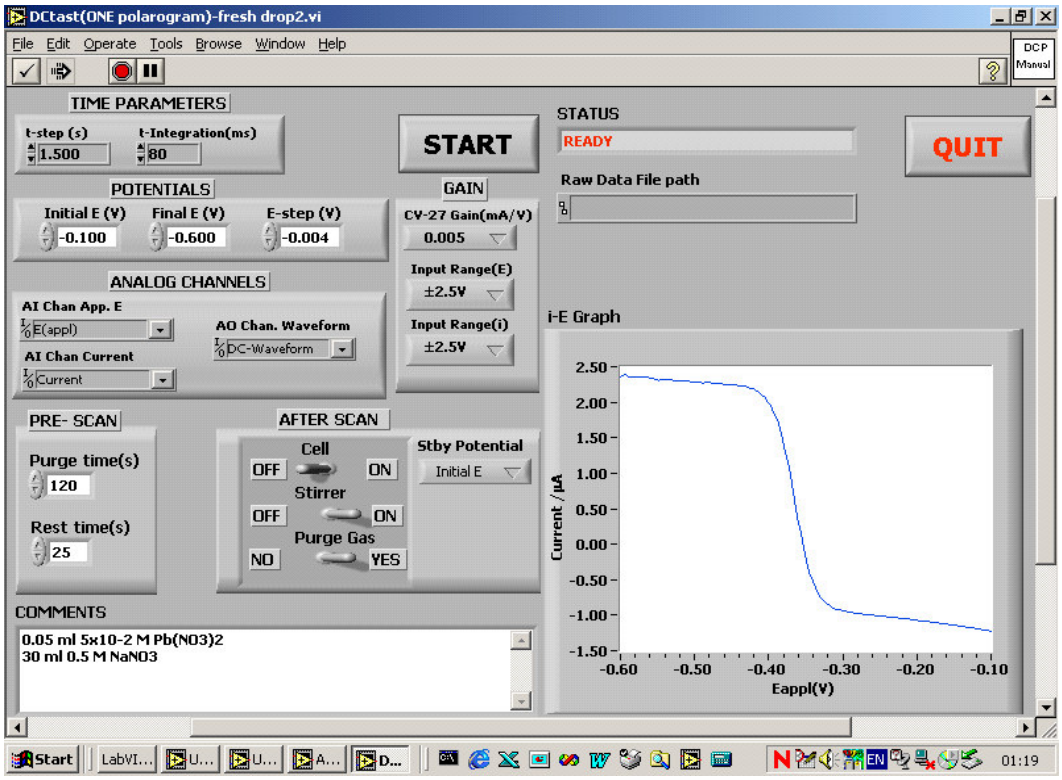


Figure 4.10: The front panel (user–interface) of the *DC* (*One Polarogram*) *VI* used for single Sampled Direct Current Polarographic scans.

To achieve Sampled DC polarography with the required high precision in timing detachment of the mercury drop and the sampling of the response current at the end of the mercury drop life, the virtual instrument *DC*(*One* Polarogram) executes in such a way that measurements made for each step of the applied potential are done in a very reproducible manner. This has been achieved through the use of the high–precision Counter channel of the DAQ card (some details related these aspects were presented in section 4.2.6).

A flowchart illustrating the programmatic execution of the *DC* (*One Polarogram*) *VI* is shown in Figure 4.11.

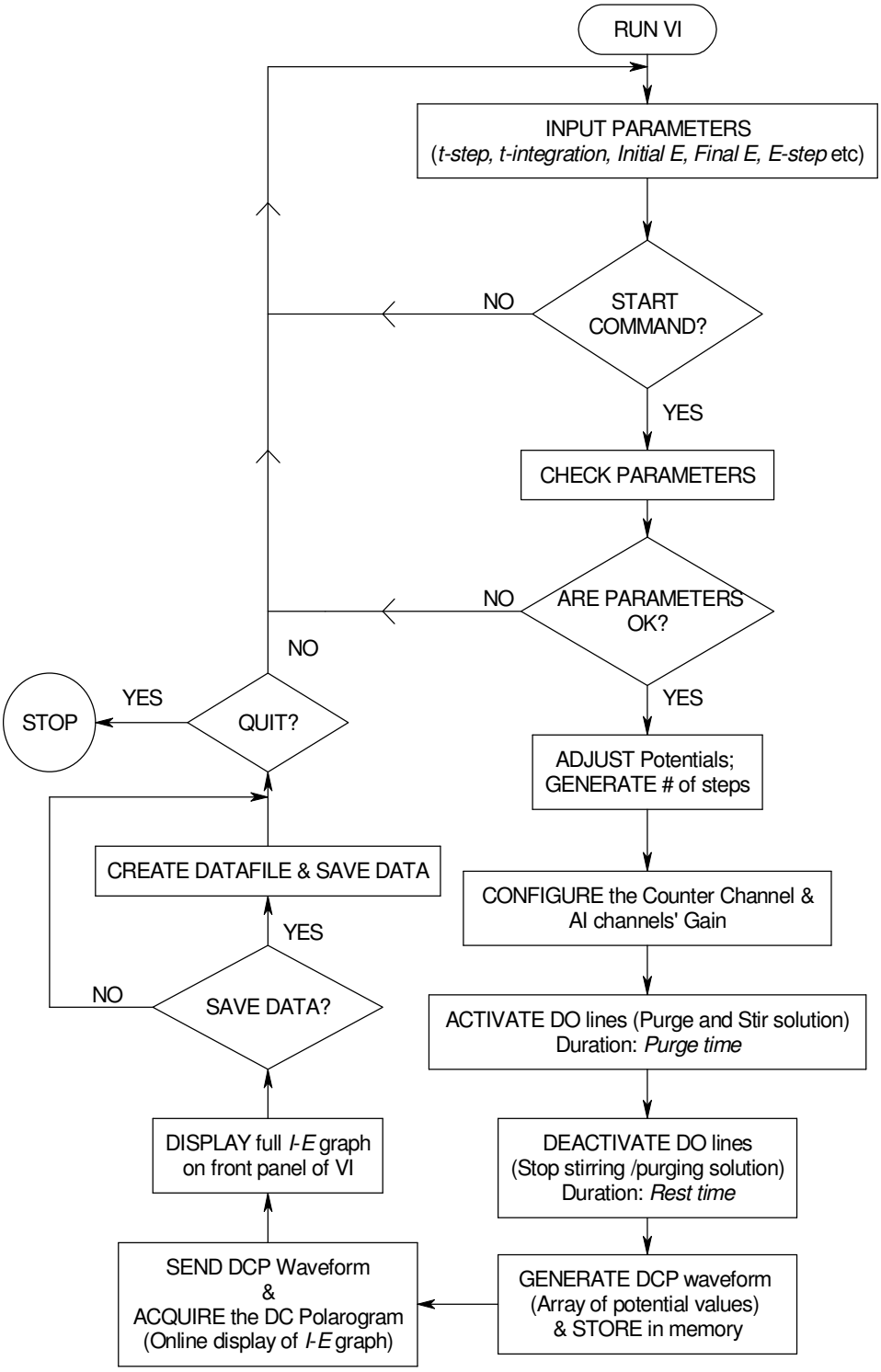


Figure 4.11: A flowchart of the *DC* (*One Polarogram*) *VI* used to generate single scans of Sampled DC polarography.

4.3.3 Sampled Direct Current Polarography with Potentiometry

Essentially, the main goal in development of an automated instrumentation in this project was to develop a unique computer–controlled instrumental set–up capable of performing automated titrations on a sample solution (with focus in metal–ligand equilibria studies) with simultaneous acquisition of both potentiometric and sampled DC polarographic data. To this end four main virtual instrument software modules, namely, *Autotitrator–DC1*, *Autotitrator–DC2*, *Autotitrator–DC–Dynamic1*, and *Autotitrator–DC–Dyanamic2*, were developed. Basically, the above–mentioned VIs were developed by combining some of the programming aspects incorporated in the VI for potentiometric titrations (*Autotitrator VI*) and that for single Sampled DC polarographic scans (*DC*(*One Polarogram VI*)) that have been described previously in sections 4.3.1 and 4.3.2, respectively. For example, monitoring of solution equilibrium potentials by the software modules proceeds in the same way as described for the *Autotitrator VI* (described in section 4.3.1). Moreover, the same programming aspects implemented for acquisition of a sampled DC polarogram used in the *DC*(*One Polarogram*) *VI* have been used.

Essentially, all of the VIs (for combined potentiometric–polarographic measurements) performed the same basic function, i.e., controlling an automated titration of a sample solution with variation in its composition (i.e. variation in pH), whereby potentiometric data as well as DCP data are acquired at appropriate titration stages, with potentiometry playing a leading role to give necessary information about homogeneous equilibration of the sample solution at a particular titration stage. In metal–ligand equilibria studies at fixed $L_T : M_T$ ratio and variable pH this role is played by GEP. Potentiometric sensors, say glass electrode, can monitor solution equilibrium potentials to within 0.2 mV with ease (the error in half–wave potentials in DC polarography, for instance, is expected in the range 0.5 – 1 mV). Furthermore, monitoring of solution equilibration (in time) by potentiometry is simple and cheap in implementation.

The differences in the virtual instruments *Autotitrator–DC1*, *Autotitrator–DC2*, *Autotitrator–DC–Dynamic1*, and *Autotitrator–DC–Dyanamic2* lie in the level of

optimization and feedback mechanism incorporated in them as far as the ways these software modules execute. In all of these VIs the titrant volume increment is fixed at a constant value (for this purpose the *Configure pH meter & Dosimat VI* described in section 4.3.1 would be used prior to the execution of an automated titration).

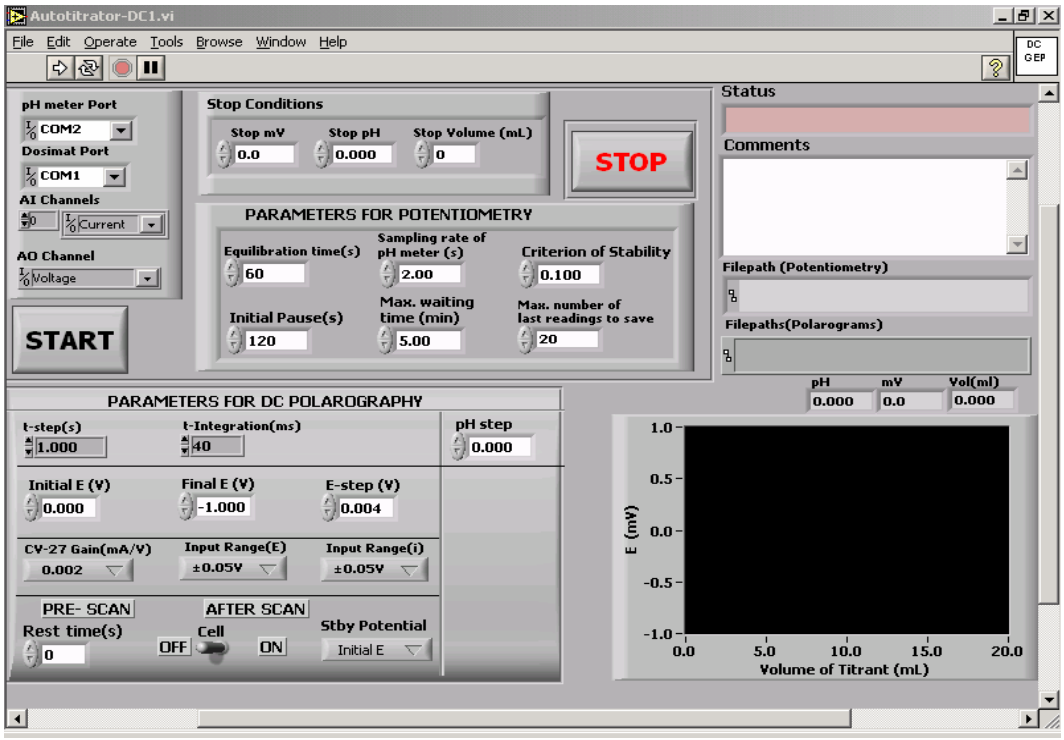


Figure 4.12: The front panel of the *AUTOTITRATOR-DC1 VI*, a software module used for automated titrations with acquisition of sampled DC polarograms and potentiometric data.

The *Autotitrator-DC1 VI* was developed first and its front panel is shown in Figure 4.12. Descriptions of the parameters have been provided in Table A.5 in Appendix A. Basically, this VI executes in a way that after each titrant volume addition (which may correspond to very small changes in equilibrium potentials) solution equilibration is checked in the usual way and GEP data are acquired and saved into a data file. A parameter called *pH Step* was introduced to the software module to ensure that sampled DC polarograms are not necessarily recorded after each titrant volume addition. If such an approach were to be followed, the software module would not perform economically as it would require a great quantity of mercury and would be time–consuming in overall performance.

The feedback mechanism using the parameter *pH Step* proceeds as follows. A polarogram is recorded at the start of an automated titration (after solution equilibration has been monitored potentiometrically) to provide a reference pH. Then titrant additions are made and solution equilibration checked in the usual way. After each titrant addition, the difference between the solution's pH and the reference pH (i.e. the previous pH at which a polarogram would have been recorded) is computed. If the difference is greater than or equal to the user–defined *pH Step*, then a new sampled DC polarogram would be recorded at this titration stage. Otherwise, a new titrant addition would be made and the cycle repeated until the *pH Step* criterion is met. This feedback mechanism allows for more GEP points than polarographic points (i.e. polarograms) to be acquired in a given automated titration. Figure 4.13 illustrates the feedback mechanism using the parameter *pH Step* in a typical application of the software.

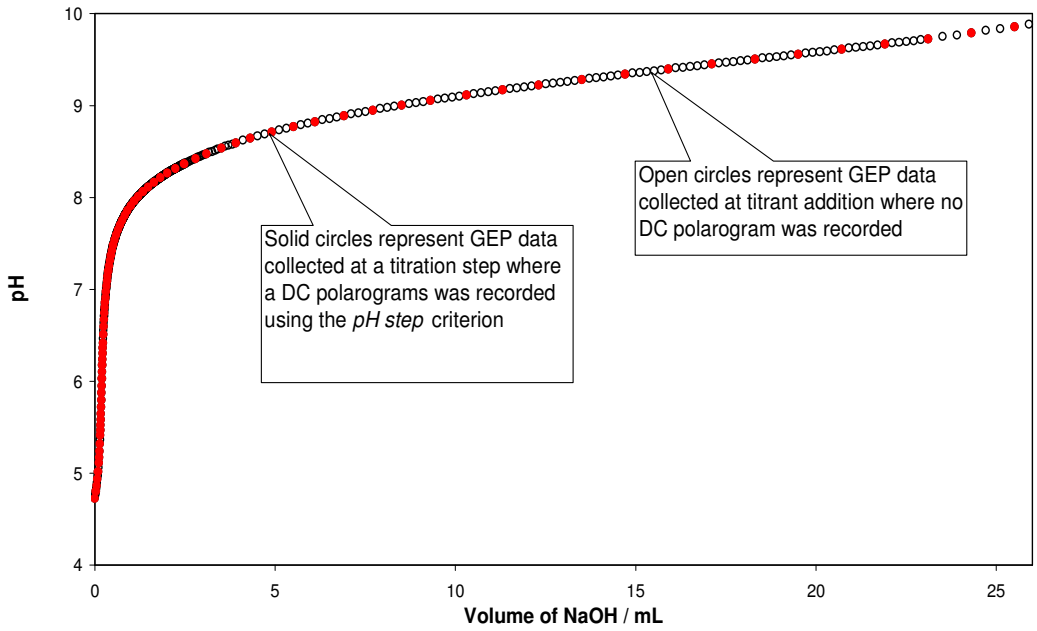


Figure 4.13: An example of a titration curve (pH versus volume of titrant) obtained from a study of Cd(II)–Glycine–OH system at fixed L_T: M_T ratio and variable pH. The experimental data were acquired automatically using the *AUTOTITRATOR–DC1 VI*. The software module allowed more GEP points to be recorded than sampled DC polarograms.

A flowchart illustrating the execution of the VI *Autotitrator–DC1* is shown in Figure 4.14.

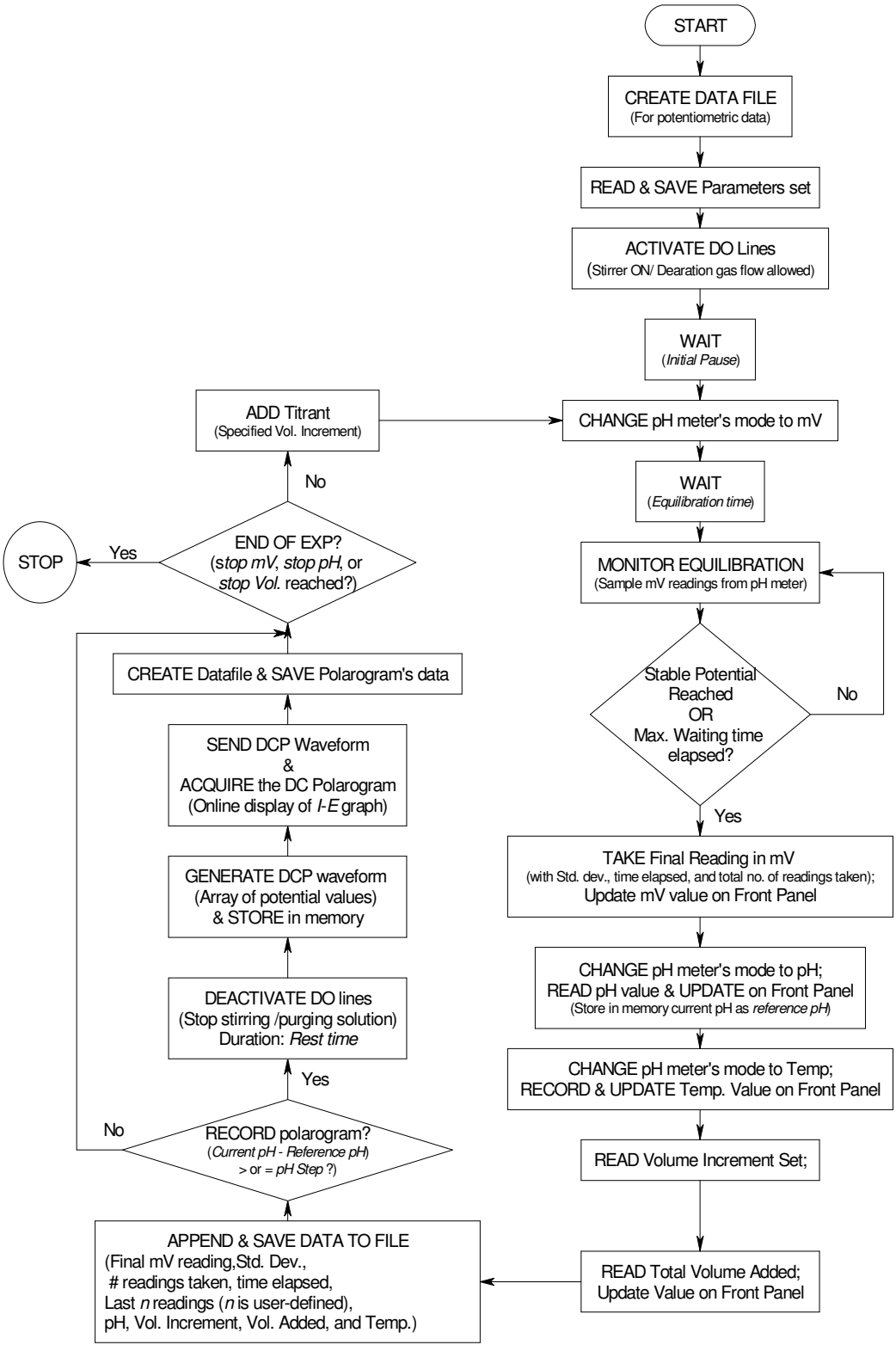


Figure 4.14: A flowchart showing programmatic execution of the *Autotitrator-DC1 VI*.

Typically, sampled DC polarographic experiments of metal–ligand systems result in shifts in the half–wave potentials (to more negative values) of recorded polarograms as a result of changes in solution composition (e.g. as pH is varied). The potential window for recording polarograms in the *Autotitrator-DC1 VI* (initially defined by the parameters *Initial E* and *Final E*) remains fixed (at the user–defined values) throughout the entire automated experiment. For instance, a user may not have prior knowledge of how much the half–wave potentials would shift during an experiment, the user would either have to unnecessarily enter a wide potential window (an approach that would consume great quantities of mercury) or incorrectly choose a potential range that would be appropriate at some stages of the experiment and inappropriate at other stages at which the shift in half–wave potentials may be significant. To this end, the *Autotitrator–DC1 VI* was optimized by developing another VI (the *Autotitrator-DC2*) which controlled an automated titration in the same way as the *Autotitrator-DC1 VI* but with an additional feedback mechanism incorporated for online adjustment of the potential window for recording polarograms.

Online adjustment of the potential window for acquisition of polarograms

To achieve automatic adjustment of the *Initial E* and *Final E* values, the software would have to perform some form of online analysis of the recorded polarograms. The expected shape of a typical sampled DC polarogram is sigmoidal (or S-shaped curve). The *Autotitrator–DC2 VI* uses a numerical differentiation algorithm (supplied with the LabVIEW package) to compute the derivative of every recorded sampled DC polarogram. Given the sigmoidal shape of a sampled DC polarogram, the resulting derivative is a peak–shaped curve which has an inflexion point that is close to the half–wave potential of the original polarogram. The E_{appl} value corresponding to the inflexion point of the derivative of a polarogram is taken by the software as an estimate of the $E_{1/2}$ value for that particular polarogram.

For purposes of adjusting the potential window, a reference $E_{1/2}$ is obtained for the first polarogram recorded. A difference of the reference $E_{1/2}$ with an estimated $E_{1/2}$

(corresponding to a given polarogram recorded at a titration stage) is computed and compared to a user–defined parameter called *Adjust Factor*. If the computed difference is greater than or equal to the *Adjust Factor* value, then adjustment of the *Initial E* and *Final E* takes place for use in recording the following polarogram. The new values of *Initial E* and *Final E* are computed using three other user–defined parameters, *IE Adjust Value*, *FE Adjust Value*, and *No. pts to search* $E_{1/2}$ (descriptions of the parameters for the *Autotitrator–DC2 VI* have been given in Table A.6 in Appendix A). Basically, the new potential values are computed using Equations 4.1 and 4.2 as follows:

$$\textit{Initial E} = \text{Estimated } E_{1/2}(\text{current polarogram}) + \textit{IE Adjust Value} \qquad \textbf{(4.1)}$$

$$\textit{Final E} = \text{Estimated } E_{1/2}(\text{current polarogram}) - \textit{FE Adjust Value} \qquad \textbf{(4.2)}$$

An example of how online adjustment of the *Initial E* and *Final E* values took place in a typical experiment is shown in Figure 4.15. In the example shown, the initial parameters were: *Initial E* = –0.200 V, *Final E* = –0.500 V, *Adjust Factor* = 20 mV, *IE Adjust Value* = 0.150 V, *FE Adjust Value* = 0.150 V, *No. pts. to search* $E_{1/2}$ = 100. It is evident from Figure 4.15 that the software module *Autotitrator-DC2 VI* detected shifts in estimates of $E_{1/2}$ values by more than 20 mV (using the criterion *Adjust Factor*) as pH was increasing. The software module automatically adjusted the *Initial E* and *Final E* values accordingly to achieve a potential window of *Estimated* $E_{1/2}$ ± 0.150 V. For instance, if no adjustment of the potential window took place, the polarogram recorded at pH 8.894 would have consisted of many background points from –0.200 V to about –0.450 V and very few points in the limiting region about –0.490 to –0.500 V. Such a polarogram would have provided few data points, for example for use in curve–fitting operations, to obtain accurate values of $E_{1/2}$ and the limiting diffusion current (the values needed for refinement operations in computation of stability constants).

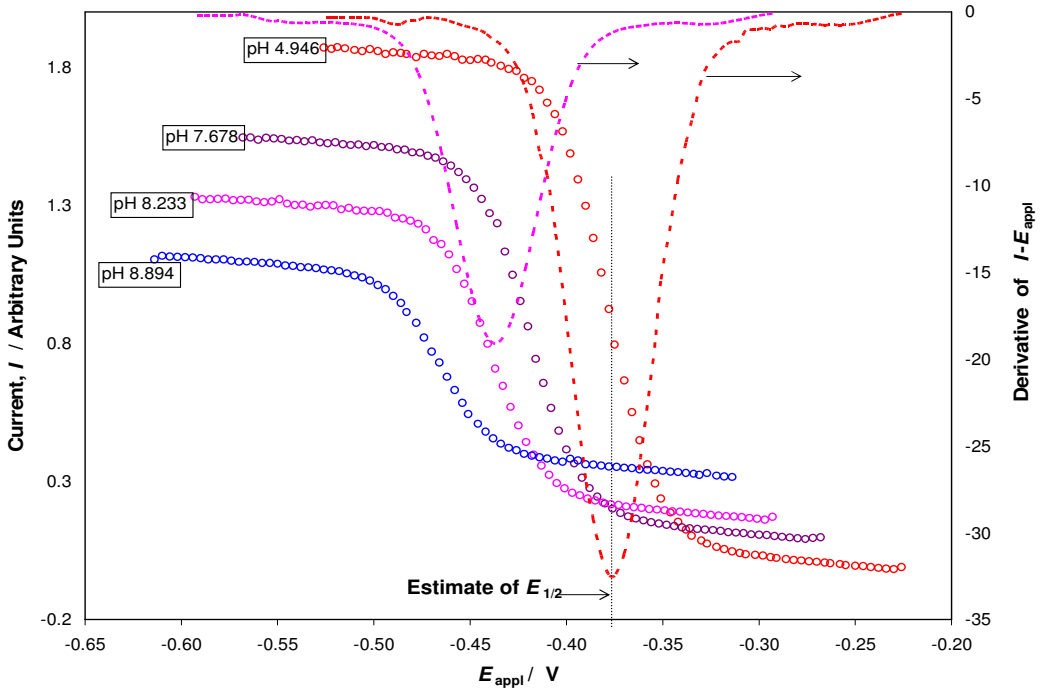


Figure 4.15: Examples of recorded Sampled DC polarograms using the *Autotitrator-DC2 VI* used in an automated potentiometric–polarographic experiment of Pb(II)–Glycine–OH system at a fixed L_T:M_T ratio and variable pH. Adjustment of *Initial E* and *Final E* values was automatically performed by the software module as the experiment progressed and the shifts in $E_{1/2}$ values were detected.

The glass electrode potentiometric data, collected on the same experiment as polarographic data in a metal–ligand equilibria study, are usually not useful for purposes of refinement operations with the final aim of computing stability constants using dedicated potentiometric software. This arises due to the fact the L_T : M_T ratios are usually high in polarographic experiments of metal–ligand systems (typically L_T : M_T ratios above 30) whereas GEP data are typically collected at L_T : M_T ratios below 10). With this in mind, the additional virtual instruments *Autotitrator–DC–Dynamic1* and *Autotitrator–DC–Dynamic2* were developed for use in metal–ligand equilibria studies by sampled DC polarography whereby only the polarographic data would be subjected to refinement operations with the final aim of arriving at a plausible model and computation of stability constants. Basically, these VIs acquired sampled DC polarograms at a faster rate compared to the VIs *Autotitrator–DC1* and *Autotitrator–DC2* by changing

solution composition (pH) in a rapid manner to achieve the desired *pH Step* (defined by the user).

The rapid change in pH (for purposes of acquiring a polarogram) is achieved as follows. Equilibrium potentials (measured potentiometrically) are not necessarily monitored after every titrant addition. Proper equilibrium potentials are monitored only after a rapid adjustment of pH to achieve a change in pH more or less required for recording polarograms (rapid attainment of the parameter *pH Step*). Proper equilibrium potentials are monitored after this rapid adjustment and polarograms recorded and saved in the usual way. The difference between *Autotitrator–DC–Dynamic1* and *Autotitrator–DC–Dynamic2* is essentially the same as difference between *Autotitrator–DC1* and *Autotitrator–DC2*. *Autotitrator–DC–Dynamic1* does not incorporate the feedback mechanism for online adjustment of the potential window for recording sampled DC polarograms whereas *Autotitrator–DC–Dynamic2* does incorporate this functionality. The front panel of *Autotitrator–DC–Dynamic2 VI* is shown in Figure 4.16, the corresponding flowchart illustrating the programmatic execution of it is shown in Figure 4.17. Table 4.2 provides a summary of the main functionalities of the software modules used for combined potentiometric–polarographic experiments.

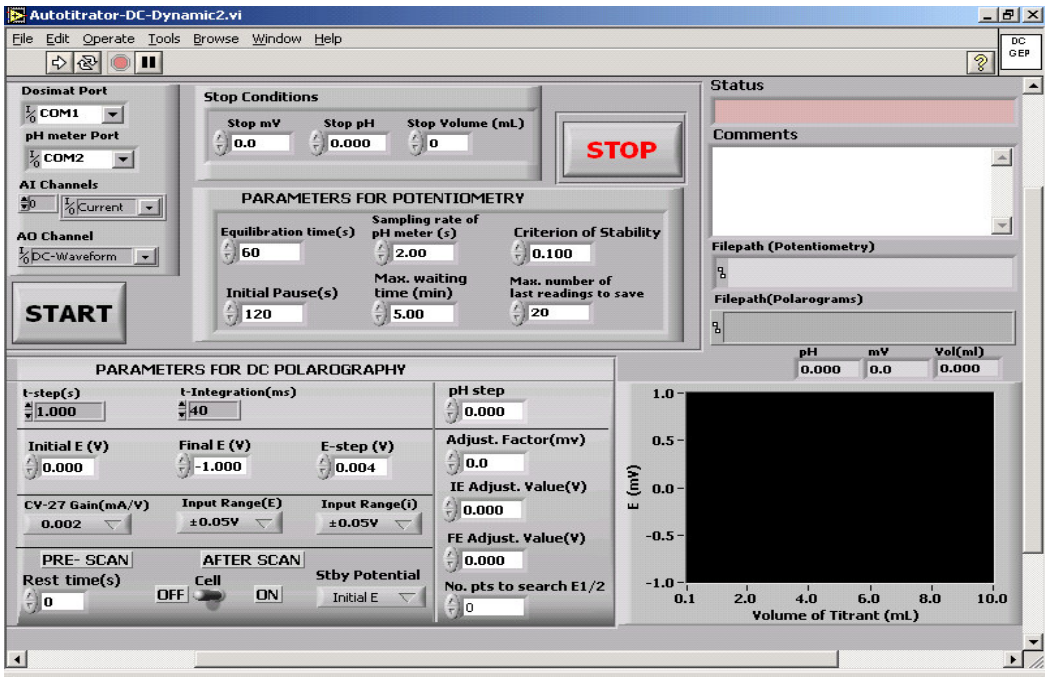


Figure 4.16: The front panel of the *AUTOTITRATOR-DC-DYNAMIC2 VI*.

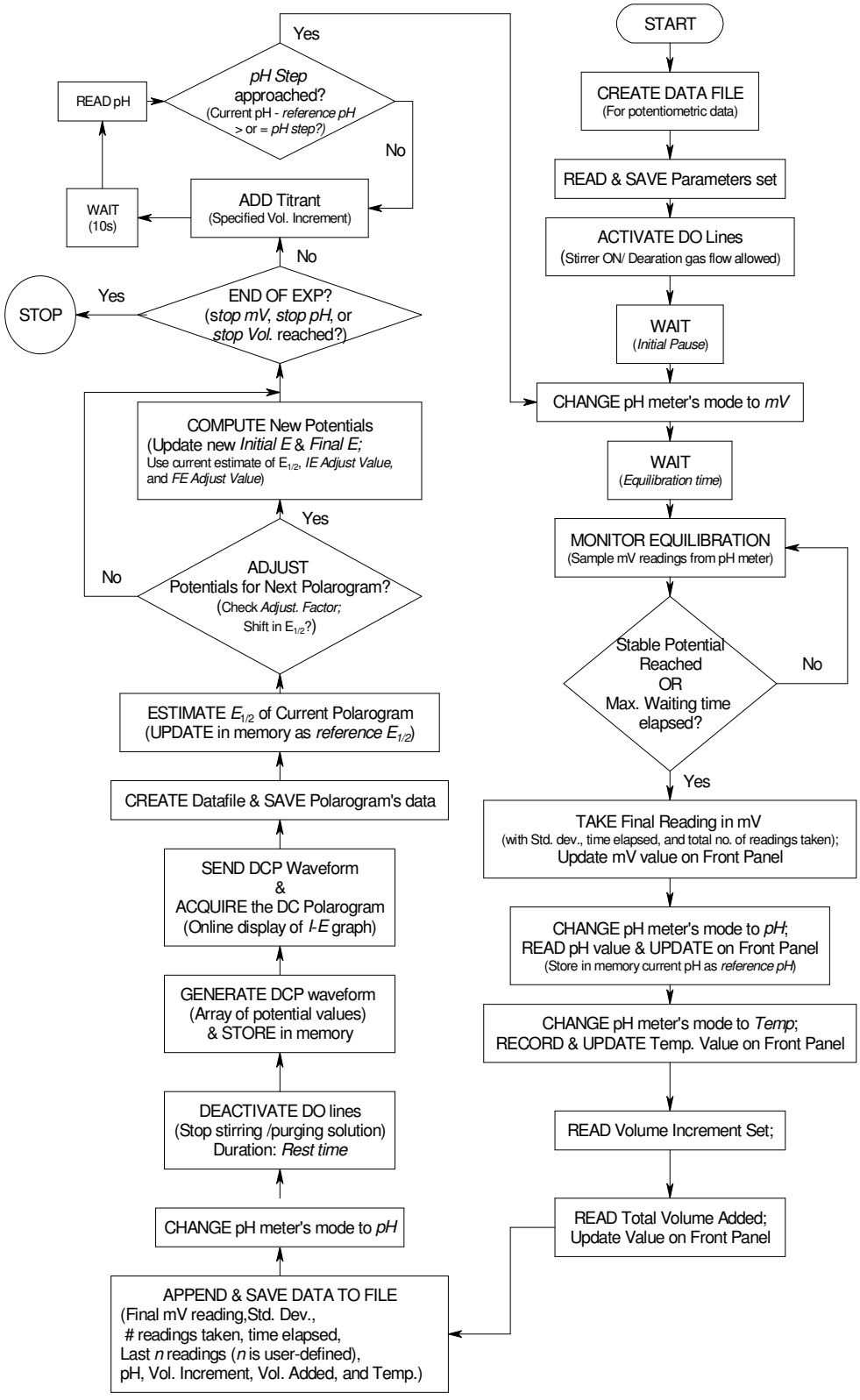


Figure 4.17: A flowchart showing the programmatic execution of the VI *Autotitrator-DC-Dynamic2*.

Table 4.2 A summary of the main features of the virtual instruments used for automated titrations with combined Sampled DCP and Potentiometric measurements on a sample solution.

Software module	**Main features**
Autotitrator-DC1	i. Fixed titrant volume increment. ii. At each titrant addition equilibrium potentials (measured potentiometrically) are monitored and the data saved. iii. Sampled DC polarograms are not necessarily recorded after each titrant addition. Polarograms are recorded based on pH changes at a user-defined rate (the parameter *pH Step* is used). iv. Same potential window used in recording all polarograms, i.e., *Initial E* and *Final E* parameters (as entered by the user) are fixed for the entire experiment. v. The number of recorded polarograms is smaller than the number of potentiometric data points acquired.
Autotitrator-DC2	i. Fixed titrant volume increment. ii. Same as in point (ii) for *Autotitrator-DC1 VI.* iii. Same as in point (iii) for *Autotitrator-DC1 VI.* iv. Online adjustment of the potential window for recording polarograms depending on the shift in estimates of $E_{1/2}$ values. v. Same as in point (v) for *Autotitrator-DC1 VI.*
Autotitrator-DC-Dynamic1	i. Fixed titrant volume increment. ii. Equilibrium potentials (measured potentiometrically) are not necessarily monitored after every titrant addition. Proper equilibrium potentials are monitored only after a rapid adjustment of pH to achieve a change in pH more or less required for recording polarograms (rapid attainment of the parameter *pH Step*). iii. Sampled DC polarograms are recorded after the appropriate pH change (when the *pH Step* condition is met). iv. Same as in point (iv) for *Autotitrator-DC1 VI.* v. The same numbers of recorded polarograms as there are potentiometric points are acquired and saved in files.
Autotitrator-DC-Dynamic2	i. Fixed titrant volume increment. ii. Same as in point (ii) for *Autotitrator-DC-Dynamic1 VI.* iii. Same as in point (iii) for *Autotitrator-DC-Dynamic1 VI* iv. Online adjustment of the potential window for recording polarograms depending on the shift in estimates of $E_{1/2}$ values. v. The same numbers of recorded polarograms as there are potentiometric points are acquired and saved in files.

4.4 VALIDATION AND PERFORMANCE OF INSTRUMENTATION

For purposes of validation and checking the performance of the computer–controlled instrumentation developed, several glass electrode potentiometric and sampled DC polarographic experiments, involving the solution equilibria of the ligand glycine (2–aminoethanoic acid) and the metal ion Cd^{2+}, were conducted.

The ligand glycine and the metal ion Cd^{2+} were selected due to the fact that they were easily accessible (cheap) and have relatively simple chemistry when studied by potentiometry and polarography. Furthermore, the solution equilibria of Cd^{2+} with glycine are well–established in the literature; hence, a direct comparison of results obtained from the validation experiments with the literature data was plausible.

4.4.1 Glass Electrode Potentiometry: Automated Titrations

The virtual instrument for automated potentiometric titrations, *Autotitrator VI*, was tested and validated by using it to perform automatic titrations in GEP experiments to study ligand protonation equilibria as well as metal–ligand equilibria.

4.4.1.1 Protonation Equilibria for Glycine

The ligand glycine is a simple amino acid that occurs naturally in living systems and plays significant roles in biochemistry of most living organisms as well as in the aquatic natural environments, such as, the marine ecosystem [18]. The chemical structure of the ligand glycine is presented in Figure 4.18.

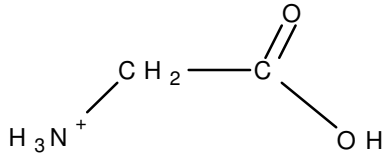


Figure 4.18: The chemical structure of a fully–protonated glycine molecule.

The ligand glycine has been extensively studied to determine the protonation equilibria in aqueous solutions at various temperatures and ionic strengths by various techniques. Glass electrode potentiometry has been the most applied technique in such studies. The fully–protonated glycine cation, $[H_2L]^+$, contains two ionisable hydrogen ions, which dissociate stepwise in fully separated processes. Depending on the pH of a solution, glycine can exist in three different forms: cationic $[H_2L]^+$, zwitterionic [HL], and anionic L^-. In acidic solutions (pH 2 – 3), the carboxyl group ($–CO_2H$) is deprotonated. In basic solutions (pH 9 – 10) the amino group ($–NH_3^+$) loses a proton to give L^- [18].

The ligand glycine provided a good reference point in the validation of the *Autotitrator VI* developed in this project to perform an automated potentiometric titration with constant titrant volume additions. For purposes of validation and checking the performance of the instrumentation, protonation constants for the ligand glycine were determined at the ionic strength of 0.5 M in $NaNO_3$ medium and at 25 °C. At least two automated titrations, corresponding to different total ligand concentrations, were performed.

The ligand glycine has two protonation constants. In the automated potentiometric titrations performed on the ligand glycine, a total of about 300 points were collected in each titration. The volume increment was set at 0.1 mL. The titrations were carried out from an initial pH of about 2 and the duration of a titration was about four hours. Experimental data from the automated titrations performed on the ligand glycine, and the corresponding results of the refinement operations for computation of the protonation constants, have been documented in Appendix B. Figure 4.19 shows a titration curve obtained from one of the automated titrations.

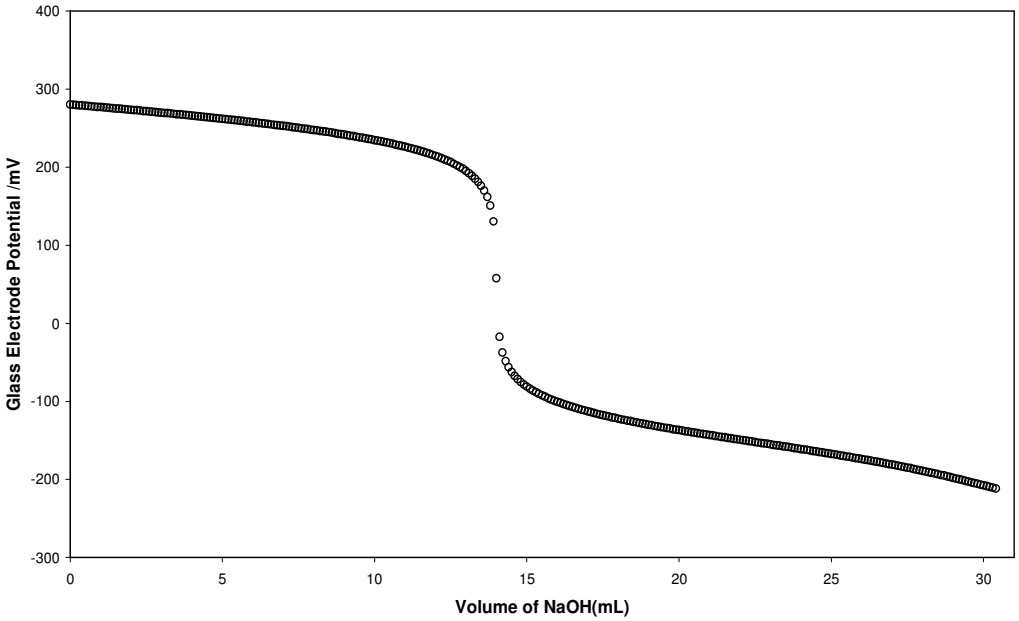


Figure 4.19: A titration curve obtained from the titration of a glycine solution with 0.05 M NaOH. Experimental Conditions: Initial $[L_T]$ =1.7980 × 10^{-2} M; Ionic strength of 0.5 M in $NaNO_3$ aqueous medium, Temperature = 25 ^oC.

Table 4.3 provides a summary of the output of the refinement procedures performed (using the ESTA suite of programs described in Chapter 3 section 3.2), to get the most reliable protonation constants for glycine from the experimental data obtained using the instrumental set–up developed and the *Autotitrator VI*. Indeed, very good agreement between the protonation constants obtained from our experiments and those reported in literature is observed. It should be noted that in the protonation equilibria experiments performed some amount of standardized acid was added to adjust the initial pH to a value of about 2. This was necessary if the second protonation constant (Log K ~ 2.3) was to be successfully determined. The addition of acid might have introduced some experimental error. Since the software used for refinement operations (ESTA) allows for simultaneous refinement of protonation constants with refinement of other experimental parameters, the initial acid concentration was refined to check if any significant error was introduced. The refined acid concentration values changed by less than 0.3 % and a better agreement between the protonation constants and the literature data was obtained (see Table 4.3C).

Table 4.3 **(A)** Dissociation constant for water (fixed in the refinement operations). **(B)** Summary of protonation constants for the ligand glycine obtained from refinement operations of GEP data collected using the automated potentiometric instrumental set–up developed in this project at 25 ˚C and ionic strength of 0.5 M in $NaNO_3$. **(C)** Summary of results from refinement operations that included refinement of initial acid concentrations.

(A)

Equilibrium	**Log *β***	**Reference**
$H^+ + OH^- \leftrightarrow H_2O$	13.74	[19]

(B)

Experimental Data	**Equilibrium**	**Log *K***	**R-Factor**	**References**
Titration 1 $[L_T] = 1.7980 \times 10^{-2}$ M	$H^+ + L^- \leftrightarrow HL$ $H^+ + HL \leftrightarrow H_2L^+$	9.573 ± 0.004 2.343 ± 0.008	0.018	This work
Titration 2 $[L_T] = 2.0664 \times 10^{-2}$ M	$H^+ + L^- \leftrightarrow HL$ $H^+ + HL \leftrightarrow H_2L^+$	9.574 ± 0.002 2.315 ± 0.004	0.009	This work
Combined refinement (Titrations 1 and 2)	$H^+ + L^- \leftrightarrow HL$ $H^+ + HL \leftrightarrow H_2L^+$	9.573 ± 0.002 2.328 ± 0.004	0.014	This work
LITERATURE DATA	$H^+ + L^- \leftrightarrow HL$ $H^+ + HL \leftrightarrow H_2L^+$	**9.54 ± 0.05** **2.39 ± 0.05**	----------	[19]

(C)

Experimental Data (Refined initial acid concentration)	**Equilibrium**	**Log *K***	**R-Factor**	**References**
Titration 1 $[L_T] = 1.7980 \times 10^{-2}$ M **Refinement of $[H^+]$:** 0.0154802 M→ 0.0155340 M	$H^+ + L^- \leftrightarrow HL$ $H^+ + HL \leftrightarrow H_2L^+$	9.591 ± 0.001 2.361 ± 0.002	0.018	This work
Titration 2 $[L_T] = 2.0664 \times 10^{-2}$ M **Refinement of $[H^+]$:** 0.0177644M → 0.0178041M	$H^+ + L^- \leftrightarrow HL$ $H^+ + HL \leftrightarrow H_2L^+$	9.587 ± 0.001 2.336 ± 0.003	0.007	This work
Combined refinement (Titrations 1 and 2)	$H^+ + L^- \leftrightarrow HL$ $H^+ + HL \leftrightarrow H_2L^+$	9.584 ± 0.001* 2.340 ± 0.002*	0.006	This work

* Protonation constants taken as final values from this work.

The protonation function, *ZBAR(H)* as defined in Chapter 3 (section 3.2, Equation 3.8), was generated using the refined protonation constants. An example of a calculated *ZBAR*(*H*) function is shown in Figure 4.20. Very good agreement is observed between the calculated function (solid line) and the experimental data (circles). As expected and as seen from the *ZBAR(H)* plot, the ligand glycine was involved in two protonation equilibria in the pH range in which experimental data were collected.

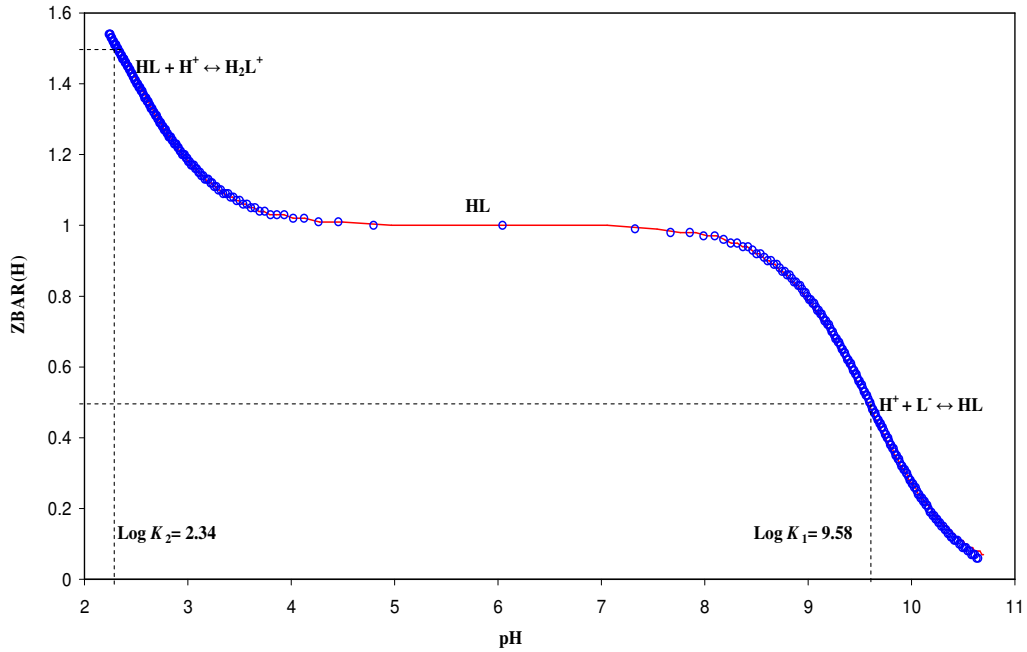


Figure 4.20: Experimental (o) and theoretical (solid line) protonation curves of the ligand glycine obtained from refinement of the GEP data collected using the automated instrumental set–up for potentiometric titrations developed in this project. Experimental conditions are as given in Figure 4.19.

4.4.1.2 A GEP study of a Cadmium(II)–Glycine–OH system

Several workers have extensively studied the cadmium–glycine system [18, 19]. The main techniques used to study this system have been potentiometry, spectrophotometry and polarography. To validate applicability of the automated titration set–up developed, for use in metal–ligand equilibria studies by potentiometry, the well established Cd(II)–Glycine–OH system was studied at

several L_T : M_T ratios (1 : 1, 2 : 1, and 3 : 1) and ionic strength of 0.5 M in $NaNO_3$ at 25 ˚C by GEP. The GEP data were acquired between pH of about 5 to 8.5 for the experiments involving the L_T : M_T ratios 1 : 1 and 2 : 1 and between pH 5 and 9.0 for the experiment involving L_T : M_T ratio 3 : 1. Fixed volume additions of between 0.01 and 0.05 mL were used. Large numbers of experimental points were acquired (between 200 and 300 points in a given automated experiment).

The ESTA suite of programmes (described in Chapter 3, section 3.2) was used for refinement operations to evaluate stability constants of plausible metal complexes. During the refinement procedures; overall stability constants of cadmium complexes, the hydrolysis constants of cadmium, and protonation constants of glycine (compiled from literature [19]) were introduced as fixed parameters. Table 4.4 gives a summary of the results obtained from the various refinement operations carried out to get the best estimates of stability constants. Different models were tried involving M(HL), ML, ML_2, ML_3, ML(OH) and ML_2(OH). The complex M(HL) was rejected in refinement operations when included in any model. In the literature the species M(HL) was only reported from polarographic studies that were carried out at relatively large L_T : M_T ratios that are not suitable for GEP experiments. It seemed plausible to conclude that at the GEP experimental conditions employed in this work, formation of the complex M(HL) was negligible, hence, the difficulties in refinement of the models that included M(HL). Thus, this species was removed from further refinement operations.

Simultaneous refinement of the stability constants for ML(OH) and ML_2(OH) could not be refined by ESTA. The complex ML(OH) was not reported in the literature, but good evidence for its formation was indicated by the 'backfanning' feature observed on the complex formation curves *ZBAR*(*M*) versus pL (described in Chapter 3, section 3.2), particularly at low L_T : M_T ratios (1 : 1 and 2 : 1). Figure 4.21 shows the potentiometric complex formation curves (*ZBAR*(*M*) versus pL = –Log [L^-]).

Table 4.4 (A) Protonation constants for the ligand glycine (L^-), dissociation constant for water and overall stability constants for Cd(II) complexes with OH^- included in the Cd(II)–L–OH model and used in the refinement procedures for GEP data. **(B)** Overall stability constants for Cd(II) with glycine from the literature and found in this work by GEP at 25 °C and ionic strength, μ = 0.5 M ($NaNO_3$).

(A)

Equilibrium	Log β	Equilibrium	Log β
$H^+ + OH^- \leftrightarrow H_2O$	13.74	$Cd^{2+} + OH^- \leftrightarrow Cd(OH)^+$	3.9
$H^+ + L^- \leftrightarrow HL$	9.54	$Cd^{2+} + 2OH^- \leftrightarrow Cd(OH)_2$	7.7
$2H^+ + L^- \leftrightarrow H_2L^+$	11.93	$Cd^{2+} + 3OH^- \leftrightarrow Cd(OH)_3^-$	10.3
		$Cd^{2+} + 4OH^- \leftrightarrow Cd(OH)_4^{2-}$	12.0
		$2Cd^{2+} + OH^- \leftrightarrow Cd_2(OH)^{3+}$	5.06
		$4Cd^{2+} + 4OH^- \leftrightarrow Cd_4(OH)_4^{4+}$	23.7

(B)

$L_T : M_T$ ratio	$[M_T]$ (M)	Log β						Hamilton R–Factor	References
		M(HL)	ML	ML_2	ML_3	ML(OH)	$ML_2(OH)$		
1 : 1	7.771×10^{-3}	Excluded	4.155 ± 0.003	Excluded	Excluded	9.470 ± 0.006	Excluded	0.01	This work
2 : 1	4.524×10^{-3}	Excluded	4.109 ± 0.004	7.67 ± 0.01	Excluded	9.79 ± 0.02	Excluded	0.03	This work
2 : 1	4.524×10^{-3}	Excluded	4.10 ± 0.02	7.34 ± 0.05	Excluded	9.47 (fix)	10.59 ± 0.07	0.02	This work
3 : 1	1.405×10^{-3}	Excluded	4.116 ± 0.002	7.588 ± 0.005	9.98 ± 0.02	9.27 ± 0.01	Excluded	0.003	This work
3 : 1	1.405×10^{-3}	Excluded	4.089 ± 0.002	7.422 ± 0.002	9.76(fix)	9.47 (fixed)	10.62 ± 0.04	0.006	This work
Combined refinement * (1:1, 2:1, 3:1)		Excluded	4.179 ± 0.002	7.321 ± 0.004	9.45 ± 0.05	9.47 ± 0.01 (fixed)	10.5 ± 0.1	0.03	This work
Literature Data [a]		Not reported	4.18	7.51	9.76	Not reported	Not reported	_____	[19]
Literature Data [b]		10.1 ±0.1	4.25 ± 0.02	7.40 ± 0.04	9.80 ± 0.04	Not reported	11.2 ± 0.1	_____	[20]
Literature Data [c]		Not reported	4.28 ± 0.18	7.72 ± 0.25	9.93 ± 0.34	Not reported	Not reported	_____	[18]

* Final model from GEP; [a] μ = 0.5 M, 25 °C, various techniques; [b] μ = 0.5 M, 25 °C, Differential Pulse Polarography; [c] μ = 0.1 – 0.5 M, 25–30 °C, various techniques

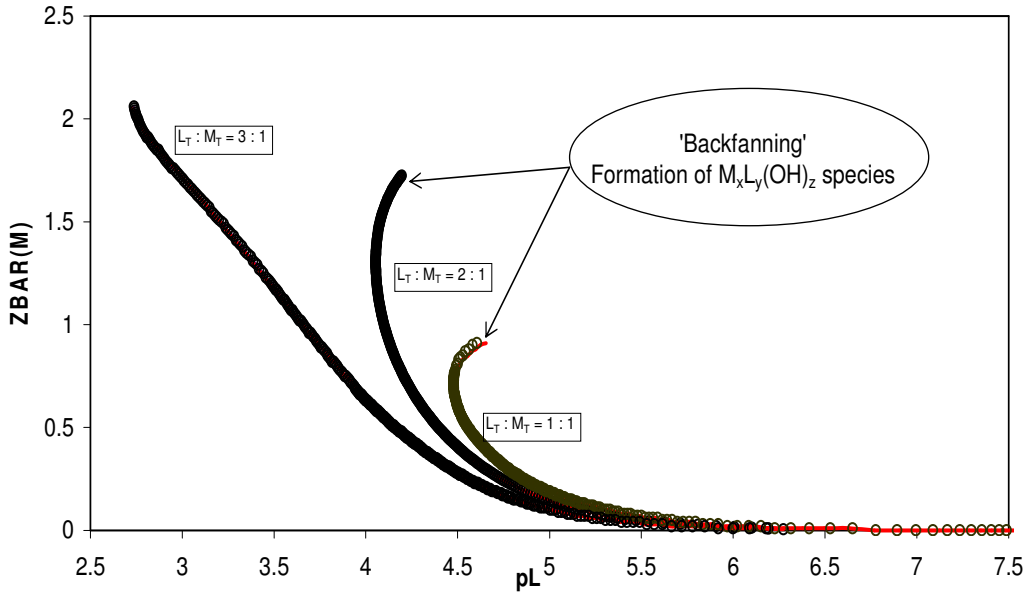


Figure 4.21: Experimental (o) and theoretical (solid line) potentiometric complex formation curves obtained for the metal–ligand models containing ML, ML_2, ML_3, ML(OH), and $ML_2(OH)$ with the optimized stability constants for these complexes obtained from the study of Cd(II)–Glycine–OH system by GEP at various $L_T : M_T$ ratios.

The *ZBAR*(*M*) functions clearly provided evidence for the formation of ML and ML_2 complexes as well as metal–ligand hydroxo species of the form $ML_x(OH)_y$. From analysis of the complex formation functions, it was difficult to conclusively provide evidence for formation of ML_3 as the *ZBAR*(*M*) function rises above the value of 2 only slightly. If ML_3 was formed then it may have formed as a minor species. Probably more data points were needed to provide more potentiometric information about formation of ML_3.

It was reasonable to include the complex ML(OH) in the refinement operations and the stability constant value obtained from analysis of the experimental data at the $L_T : M_T$ ratio of 1 :1, was taken as the most accurate value for the complex ML(OH). The final model in this work was taken from the combined refinement operation whereby all three sets of data collected at the different $L_T : M_T$ ratios were optimized simultaneously by the software ESTA. But it was necessary to maintain the stability constant for ML(OH) at the value obtained from the experimental data at $L_T : M_T$ ratio 1 : 1.

Compared to the literature data good estimates of the stability constants for the complexes ML and ML_2 were obtained. The stability constants values for $ML_2(OH)$ and ML_3 were somehow lower than the values reported in literature, but this was expected since occurrence of precipitation prevented the collection of enough experimental data points in the pH range where the formation of these species was more pronounced.

Some species distribution diagrams (Figures 4.22 and 4.23) for the Cd(II)–Glycine–OH system were generated using the values for ML, ML_2, and ML(OH) obtained in this work (final model in Table 4.4) and the values for M(HL), ML_3, and $ML_2(OH)$ taken from the literature [20]. Clearly, for the experimental conditions employed in the GEP experiments performed in this project, it was not plausible to accurately determine the stability constants for the M(HL), ML_3 and $ML_2(OH)$. It is plausible to evaluate these complexes at larger L_T : M_T ratios. Such experimental conditions are typical for polarographic studies of metal–ligand systems.

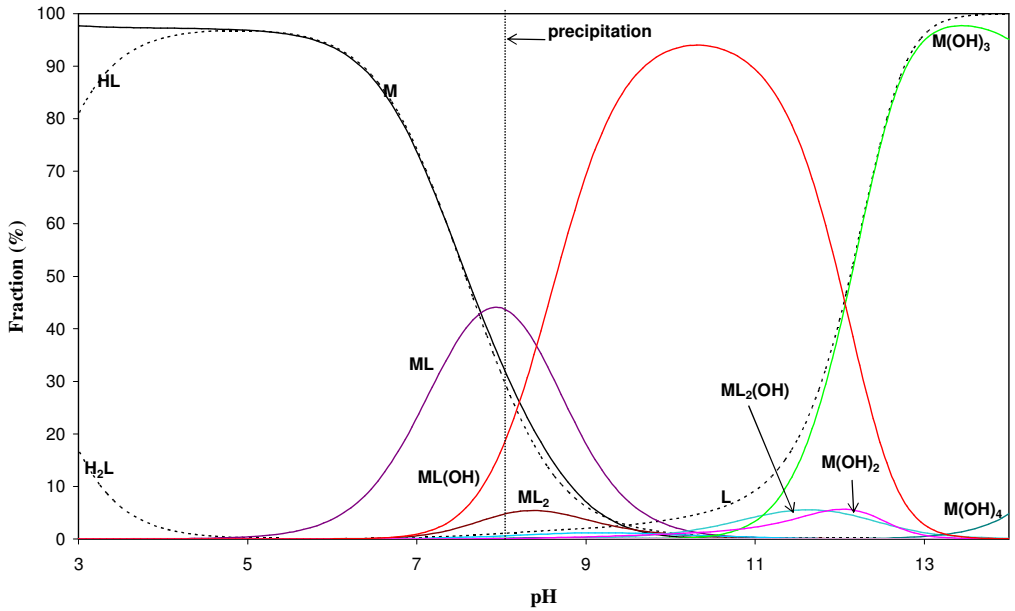


Figure 4.22: A species distribution diagram for the Cd(II)–Glycine–OH system at L_T : M_T = 1 : 1, $[M_T] = 7.771 \times 10^{-3}$ M generated using the model containing M(HL), ML, ML_2, ML_3, ML(OH) and $ML_2(OH)$. Experimental data were collected in the pH range 5 – 8.

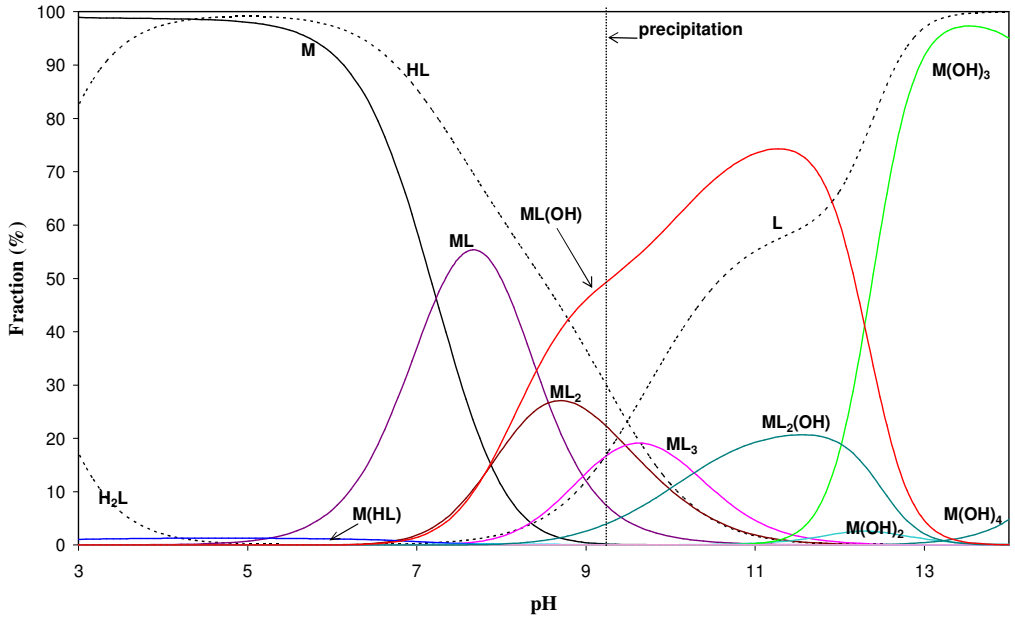


Figure 4.23: A species distribution diagram for the Cd(II)–Glycine–OH system at $L_T : M_T$ = 3 : 1, $[M_T] = 4.679 \times 10^{-3}$ M generated using stability constants from the model containing M(HL), ML, ML_2, ML_3, ML(OH), $ML_2(OH)$. Experimental data were collected in the pH range 5–9.

4.4.2 Sampled Direct Current Polarography with Potentiometry: Automated Titrations

4.4.2.1 A polarographic study of a Cadmium(II)–Glycine–OH

For purposes of validating the instrumental set–up, with regard to combined potentiometric–polarographic measurements on a sample solution, several titrations were performed (at fixed $L_T : M_T$ ratios, fixed ionic strength in aqueous medium, fixed temperature of 25 ˚C and variable pH) to study the solution equilibria of the metal–ligand system Cd(II)–glycine–OH. Glass electrode potentiometry was the leading technique in all of the experiments. It should be noted that the refinement operations employed in the evaluation of polarographic data do not include mass balance equation for the total proton concentration $[H_T]$; the free proton or hydroxide ion concentrations ($[H^+]$ or $[OH^-]$) are obtained directly from the pH measurements by the calibrated glass electrode and K_w for

water. Thus, in the automated titrations performed (with combined GEP and sampled DC polarographic measurements), the leading role played by GEP is also crucial in providing the information for $[H^+]$ or $[OH^-]$, the information that is necessary in the refinement operations of the polarographic data for evaluation of stability constants. Accordingly, sampled DC polarograms were automatically recorded at appropriate pH values using the *pH Step* software criterion (described previously in section 4.3). A set of 80 to 90 polarograms were collected in a given experiment in steps of between 0.04 and 0.1 pH units.

(*i*) *Analysis of DC polarograms*

The sampled DC curves were analysed using the curve–fitting procedure described in Chapter 3 (sections 3.5.2.2 – 3.5.3.2). The Cukrowski's curve–fitting method was used for analysis of the sampled DC polarograms collected (Equations 3.32 – 3.33). The recorded polarograms were essentially found to correspond to electrochemically reversible reduction processes at pH ranges between 4 and 8 and slightly quasi–reversible reduction processes at high pH values (8–11). The reversibility index parameter δ varied between 0.85 and 1. The curve–fitting procedure described in section 3.5.3.2 was implemented for evaluation of $E_{1/2}$ and I_d values from the DC curves for use in refinement operations performed for computation of stability constants. An illustration of typical sampled DC curves collected (and the analysis performed on them) is shown in Figure 4.24. In the example presented in Figure 4.24, it can be noted that automatic adjustment of the potential window for recording the DC polarograms was done successfully by the software module used to control the automated data acquisition.

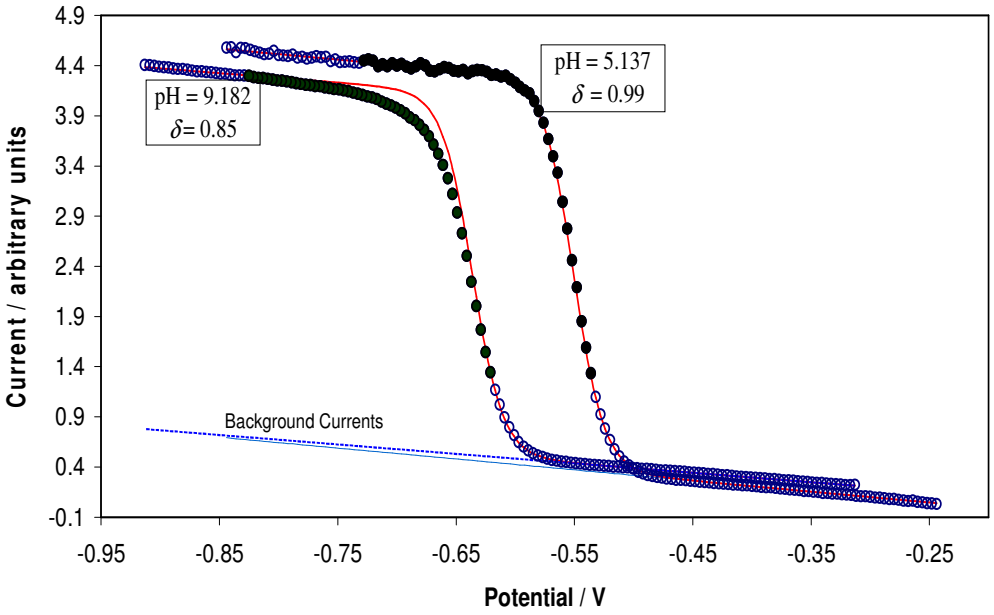


Figure 4.24: Examples of sampled DC curves recorded during a study of Cd(II)–Glycine–OH (L_T : M_T = 200 : 1(fixed) and variable pH; $[M_T] = 1.016 \times 10^{-4}$ M). An illustration of the curve–fitting operations is also shown – for details see the text. Circles (experimental points) representing the recorded current at a particular applied potential; solid lines represents theoretically fitted curves corresponding to fully reversible processes; circles with solid dots inside represent points excluded in the fitting procedure; dotted lines represent computed background currents.

(*ii*) *Modelling*

Modelling of the metal–ligand system was based on the analysis of slopes (described in Chapter 3, section 3.3.2) shown in Figures 4.25 and 4.26. In Figure 4.26, there is no significant shift in the half–wave potential up to pH of about 6.5. However, one cannot exclude the possibility of the formation of M(HL) as reduction of this species would not cause the shift in the half–wave potential. This is because the formation of M(HL) would occur in the pH range where HL is the major form of the ligand glycine and reduction of M(HL) would not involve protons. The slopes observed in Figures 4.26 and 4.27 clearly supported the formation of major metal containing species ML, ML_2 and ML_3. In Figure 4.26, above pH 9.5 the free ligand L predominates in the solution and the shift in the

half–wave potential approaches the value of about 30 mV per pH unit that indicates the formation of a metal complex containing a single OH group of the form $ML_j(OH)$.

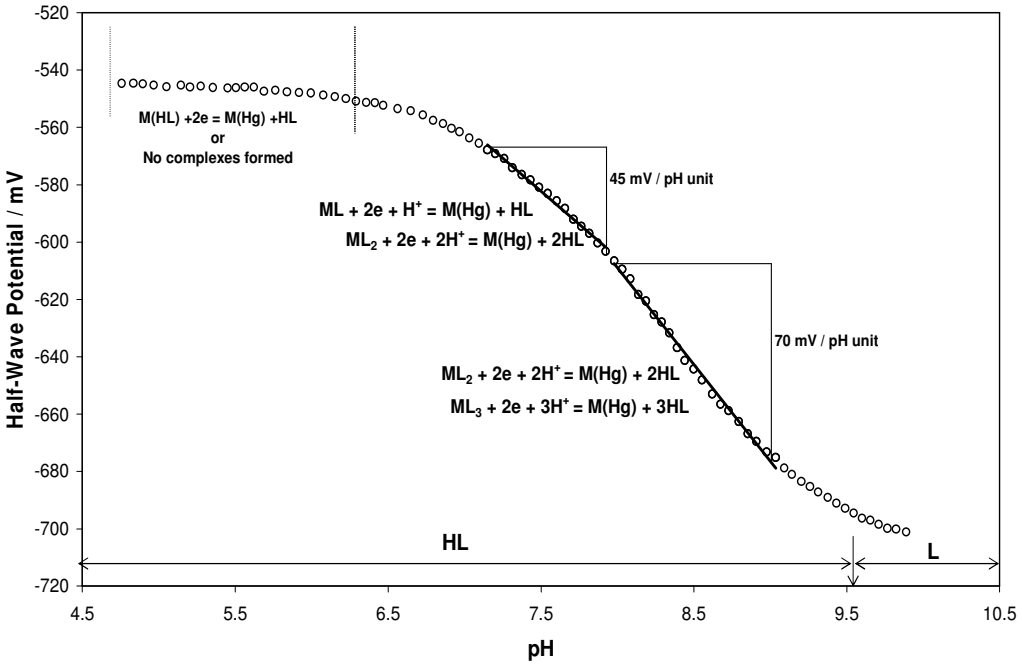


Figure 4.25: An example of interpretation of the observed shift in half–wave potential plotted against pH for the Cd(II)–Glycine–OH system studied by sampled DCP at experimental conditions as indicated for Figure 4.24.

From the above analysis, it was reasonable to assume the following metal–ligand model: M(HL), ML, ML_2, ML_3, and ML(OH), $ML_2(OH)$.

(*iii*) *Optimisation of a metal–ligand model and refinement of stability constants*

The refinement of stability constants from the sampled DC polarographic data was performed according to the methodology described in Chapter 3 (section 3.3.1). An example of the experimental complex formation curve (ECFC) and calculated complex formation curve (CCFC) plotted versus pH is shown in Figure 4.27. A summary of the results from the refinement operations and comparison of the results obtained with the literature data is presented in Table 4.5.

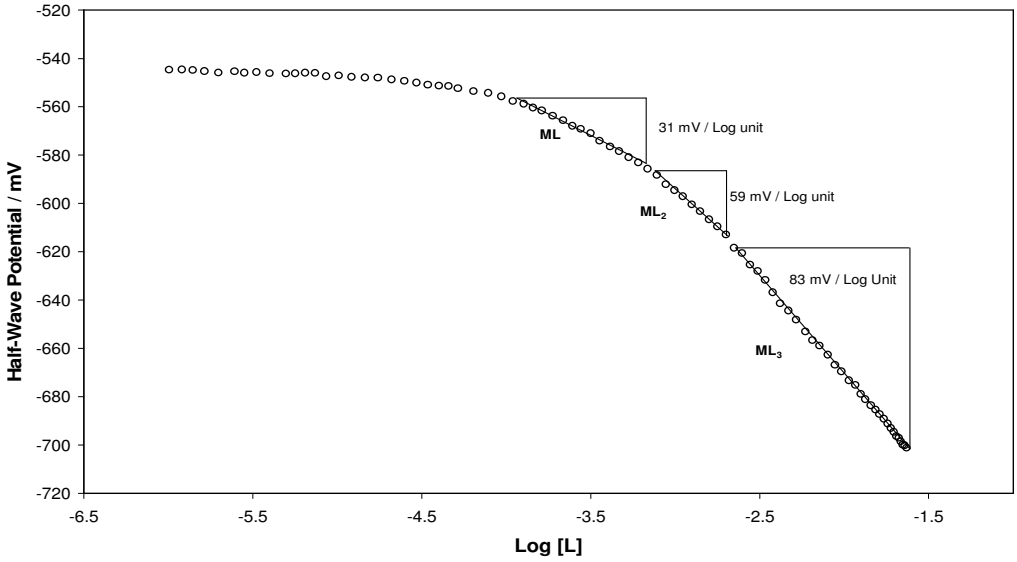


Figure 4.26: An example of interpretation of the observed shift in half–wave potential plotted against Log [L] for the Cd(II)–Glycine–OH system studied by DCP at fixed L_T : M_T ratio and variable pH at experimental conditions as indicated for Figure 4.24.

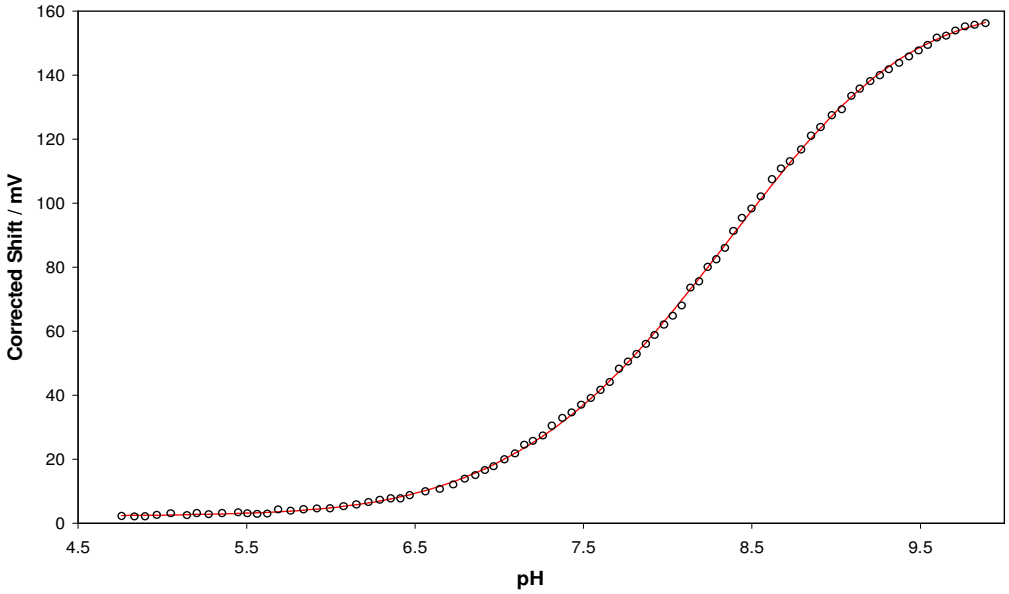


Figure 4.27: Experimental (circles) and calculated (solid line) complex formation curves obtained for the Cd(II)–Glycine–OH system studied at a fixed L_T : M_T ratio of 700; $[M_T]$ = 8.456×10^{-5} M. The curves were obtained from the final model given in Table 4.5.

During the optimization of the metal–ligand model, simultaneous refinement of the stability constants for the species ML(OH) and $ML_2(OH)$ was not possible,

some level of competition between these two species existed that made the simultaneous optimization of their stability constants rather impossible. Moreover, these hydroxyl species (at the large L_T : M_T ratios used in the polarographic studies) become major species in solution at high pH values (above 10). Also, the formation of $ML_2(OH)$ is more pronounced at large L_T : M_T ratios than the formation of ML(OH). It should be noted that not enough experimental data points were collected at pH values above 10 in the polarographic studies performed. Thus, during optimization procedures to obtain a metal–ligand model consistent with the observed literature models, it was plausible to fix the stability constant of the MLOH species at the value obtained from GEP experiments (described in section 4.4.1). Generally, good agreement between the results obtained in this work and those reported in the literature was found, particularly for the major metal species ML, ML_2, and ML_3.

Some examples of species distribution diagrams are shown in Figures 4.28 and 4.29.

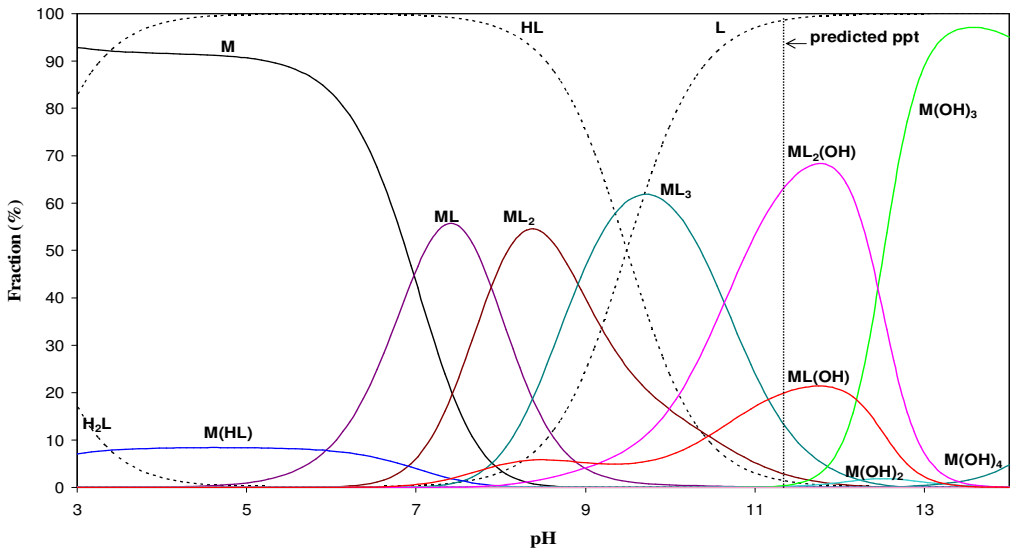


Figure 4.28: Species distribution as a function of pH for the Cd(II)–Glycine–OH system at L_T : M_T = 200; $[M_T] = 1.016 \times 10^{-4}$ M. The distribution was computed using results obtained as final model given in Table 4.5. Actual experimental data for this ratio were collected in the pH range 4 to 11. ppt = precipitation.

Table 4.5. (A) Protonation constants for the ligand glycine (L^-), dissociation constant for water and overall stability constants for Cd(II) complexes with OH^- included in the Cd(II)–L–OH model and used in the refinement procedures for Sampled DC polarographic data. **(B)** Overall stability constants for Cd(II) with glycine from the literature and found in this work by Sampled DC polarography at 25 °C and ionic strength of 0.5 M in $NaNO_3$. OF represents the overall fit (Equation 3.15) of complex formation curves, the computed curve in the objective experimental function. For details see the text.

(A)

Equilibrium	**Log β**	**Equilibrium**	**Log β**
$H^+ + OH^- \leftrightarrow H_2O$	13.74	$Cd^{2+} + OH^- \leftrightarrow Cd(OH)^+$	3.9
$H^+ + L^- \leftrightarrow HL$	9.54	$Cd^{2+} + 2OH^- \leftrightarrow Cd(OH)_2$	7.7
$HL + H^+ \leftrightarrow H_2L$	2.39	$Cd^{2+} + 3OH^- \leftrightarrow Cd(OH)_3^-$	10.3
		$Cd^{2+} + 4OH^- \leftrightarrow Cd(OH)_4^{2-}$	12.0
		$2Cd^{2+} + OH^- \leftrightarrow Cd_2(OH)^{3+}$	5.06
		$4Cd^{2+} + 4OH^- \leftrightarrow Cd_4(OH)_4^{4+}$	23.7

(B)

$L_T : M_T$ ratio	**$[M_T]$ (M)**	**Log β**						**OF (± mV)**	**References**
		M(HL)	**ML**	**ML_2**	**ML_3**	**ML(OH)**	**$ML_2(OH)$**		
200 : 1	1.016×10^{-4}	10.35 ± 0.08	4.23 ± 0.02	7.04 ± 0.05	9.84 ± 0.02	9.01 ± 0.05	Excluded	0.384	This Work
200 : 1	1.016×10^{-4}	10.35 ± 0.08	4.23 ± 0.02	7.16 ± 0.04	9.84 ± 0.02	9.47(fixed)	10.87 ± 0.05	0.379	This Work
600 :1	8.051×10^{-5}	10.28 ± 0.06	4.32 ± 0.02	7.42 ± 0.03	9.88 ± 0.05	Excluded	12.17 ± 0.09	0.305	This Work
600 : 1	8.051×10^{-5}	10.28 ± 0.06	4.32 ± 0.02	7.35 ± 0.03	9.89 ± 0.05	9.47 (fixed)	10.87 (fixed)	0.305	This Work
700 : 1	8.456×10^{-5}	10.05 ± 0.05	4.15 ± 0.02	7.28 ± 0.04	9.90 ± 0.01	9.47 (fixed)	10.87 (fixed)	0.496	This Work
Final Model*		**10.2 ± 0.1**	**4.23 ± 0.03**	**7.36 ± 0.06**	**9.87 ± 0.05**	**9.47 ± 0.01**	**10.87 ± 0.05**	_____	This Work
Literature Data [a]		Not reported	4.18	7.51	9.76	Not reported	Not reported	_____	[19]
Literature Data [b]		10.1 ± 0.1	4.25 ± 0.02	7.40 ± 0.04	9.80 ± 0.04	Not reported	11.2 ± 0.1	_____	[20]
Literature Data [c]		Not reported	4.28 ± 0.18	7.72 ± 0.25	9.93 ± 0.34	Not reported	Not reported	_____	[18]

*Averaged values from the various models, Log β for MLOH taken from GEP results; [a], [b], [c] Same information as presented in Table 4.4.

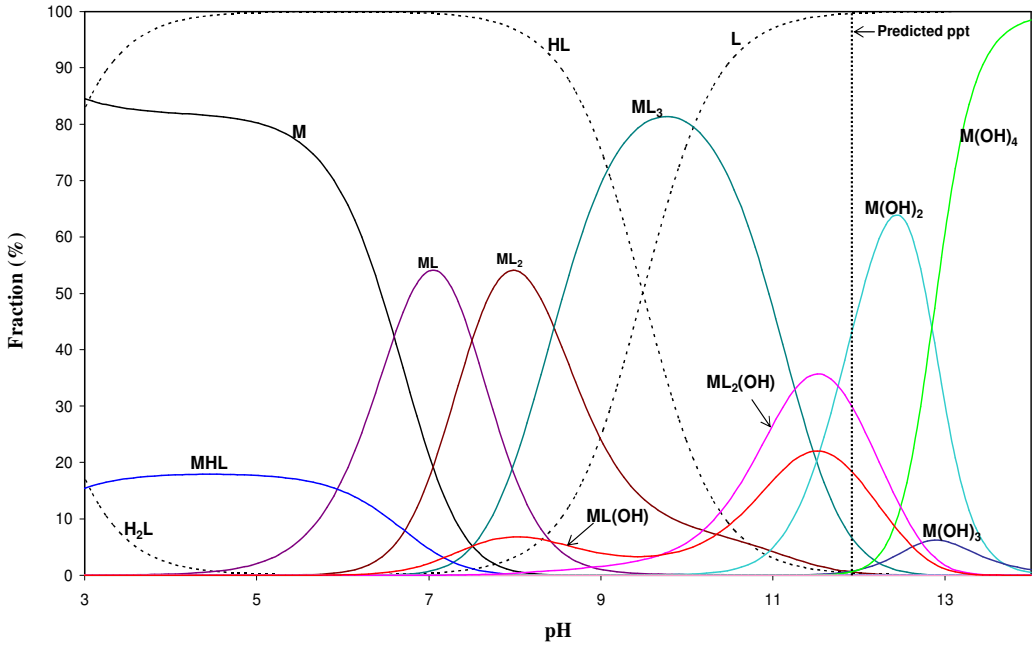


Figure 4.29: Species distribution as a function of pH for the Cd(II)–Glycine–OH system at $L_T : M_T = 600$; $[M_T] = 8.051 \times 10^{-5}$ M. The distribution was computed using results obtained as final model given in Table 4.5. Actual experimental data for this ratio were collected in the pH range 5 to 10. ppt = precipitation.

From the species distribution diagrams (Figures 4.28 – 4.29) it is seen that the major species ML, ML_2, and ML_3 are formed in a consecutive manner with large fraction for each species. The fraction of M(HL) does not vary much in the pH range between 3.5 and 6. The small fraction (less than 10 %) of M(HL) formed and the constancy in the solution composition in this pH range resulted in the very small change in the free metal ion concentration. This suggests that at low $L_T : M_T$ ratios such as used in GEP, it would be difficult if not impossible to observe the M(HL) species. It is also evident from the species distribution diagram (Figure 4.28) that MLOH begins to form at a pH of about 7 and remains a minor species compared to ML_2, ML_3 and $ML_2(OH)$. The species distribution is in support of the difficulties encountered in simultaneous optimization of the stability constants for ML(OH) and $ML_2(OH)$ during the refinement operations performed on the polarographic data.

4.5 CONCLUSIONS

In this chapter, description of a computer–controlled instrumental set–up, developed in this research project (with particular applications in solution equilibria studies) was described. The instrumental set–up had capabilities of performing automated titrations on a sample solution whereby potentiometric and sampled DC polarographic measurements could be made independently or potentiometric and sampled DC polarographic measurements could be made in a combined fashion. The methodology of virtual instrumentation was implemented to achieve a low–cost instrumental set–up with the required capabilities. In this regard, several LabVIEW–based virtual instruments were developed with different functionalities depending on the level of feedback mechanisms incorporated in them for controlling automated titrations.

For purposes of validating and checking the performance of the instrumental set–up as well as showing examples of its applications in solution equilibria studies, the solution equilibria of the ligand glycine and the metal ion Cd^{2+} were elucidated by glass electrode potentiometry and sampled DC polarography. Protonation constants for the ligand glycine and stability constants of several complexes of Cd^{2+} with glycine were determined. Good agreement between the results obtained in this work and literature data were found.

Large numbers of experimental points were acquired in the experiments performed which would not be conveniently obtained by manual methods. The instrumental set–up increased versatility and convenience in performing experiments involving metal–ligand equilibria by sampled DC polarography (with potentiometry as a leading technique).

4.6 REFERENCES

1. J. K Foreman and P. B. Stockwell, *Automatic Chemical Analysis*, Sussex: Ellis Horwood, **1975**.
2. National Instruments LabVIEW, *Measurements Manual*, July 2000 ed. National Instruments: Austin, Texas, **2000**.
3. G. W. Johnson, *LabVIEW Graphical Programming: Practical Applications in Instrumentation and Control*, New York: McGraw Hill, **1994**.
4. J. P. Walters, *Analytical Chemistry*, vol. 67, 1995, pp. 34A-35A.
5. A. Economou, S. D. Bolis, C. E. Efstathio, G. J. Volikakis, *Anal. Chim. Acta*, Vol. 467, **2002**, pp. 179 – 188.
6. LabVIEW™, National Instruments, 6504 Bridge Point Parkway, Austin, Texas 78730-3039, USA. http://www.ni.com.
7. M. Anderson, *Data Flow Programming with Labview*, National Instruments (Application note PN 320117-01), **1988**.
8. Metrohm, *Instructions for Use for* 780 *pH meter*, 1st ed., Metrohm Ltd., CH-9101 Herisau, Switzerland, **2002**.
9. G. H. Olsen, *Electronics: A Handbook for Engineers and Scientists*, 2nd Ed., London: Butterworths, **1991**.
10. Metrohm, *Instructions for Use for 765 Dosimat*, Metrohm Ltd., CH-9101 Herisau, Switzerland, **2000**.
11. *Operation/ Instruction Manual for the CV–27 Voltammograph*, **1984**, Bioanalytical Systems Inc, West Lafayette, IN, USA.
12. A. J. Bard and L. R. Faulkner, *Electrochemical Methods: Fundamentals and Applications*, 2nd ed., John Wiley& Sons: USA, **2001**.Metrohm, *Instructions for Use* 663 VA stand, Metrohm Ltd., CH-9101 Herisau, Switzerland, **1991**.
13. G. Svehla, *Automatic Potentiometric Titrations*, Oxford: Pergamon Press, **1978**.
14. P. Gans, and B. O'Sullivan, *Talanta*, Vol. 51, **2002**, pp. 33–37.
15. D. J. Leggett, *Anal. Chem.*, Vol. 50, No. 6, **1978**, pp. 718–722.
16. T. F. Christiansen, J. E. Busch, and S. C. Krogh, *Anal. Chem.*, Vol. 48, No. 7, **1976**, pp. 1051–1056.

17. A. H. B. Wu, and H. V. Malmstadt, *Anal. Chem.*, Vol. 50, No. 14, **1976**, pp. 2090–2096.
18. IUPAC Analytical Chemistry Division, Commission on Equilibrium Data, *Pure Appl. Chem.*, Vol. 63, No. 4, **1991**, pp. 597 – 638.
19. NIST Standard Reference Database 46. *NIST Critically Selected Stability Constants of Metal Complexes Data* version 7.0. Data collected and selected by R. M. Smith and A. E. Martell for US Department of Commerce, National Institute of Standards and Technology, **2003**.
20. I. Cukrowski and G. Ngigi, *Electroanalysis*, Vol. 13, No. 15, **2001**, pp. 1242–1252.